CRYSTAL GROWTH & DESIGN

Article

pubs.acs.org/crystal

Syntheses, Topological Structures, and Photoluminescences of Six New Zn(II) Coordination Polymers Based on Mixed Tripodal Imidazole Ligand and Varied Polycarboxylates

Di Sun,*[,†] Zhi-Hao Yan,[†] Vladislav A. Blatov,*[,‡] Lei Wang,[†] and Dao-Feng Sun[†]

[†]Key Lab of Colloid and Interface Chemistry, Ministry of Education, School of Chemistry and Chemical Engineering, Shandong University, Jinan, 250100, P. R. China

[‡]Department of Chemistry, Samara State University, Ac. Pavlov St. 1, Samara, 443011, Russia

Supporting Information

ABSTRACT: Solvothermal reactions of the tripodal ligand 1,3,5-tris(1-imidazolyl)-benzene (tib) and different polycarboxylates with zinc nitrate provided six new zinc(II) coordination polymers (CPs), namely, $\{[Zn_8(tib)_5(bdc)_8(H_2O)]\cdot 7DMF\cdot 18H_2O\}_n$ (**1**), $\{[Zn_3(tib)_2(bpdc)_3]\cdot 5H_2O\}_n$ (**2**), $\{[Zn(tib)(pdac)]\cdot 1.5H_2O\}_n$ (**3**), $\{[Zn_6(tib)_2(pdac)_3]\cdot DMA\cdot 2H_2O\}_n$ (**4**), $\{[Zn_2(tib)_2(pma)]\cdot 4H_2O\}_n$ (**5**), $\{[Zn_2(tib)(Htib)(H_2pma)(Hpma)]\cdot 2H_2O\}_n$ (**6**) (H_2bdc = 1,3-benzenedicarboxylic acid, H_2bpdc = 4,4′-biphenyldicarboxylic acid, H_2pdac = 1,2-phenylenediacetic acid, H_4pma = pyromellitic acid, DMF = *N*,*N*′-dimenthylformamide, DMA = *N*,*N*′-dimethylacetamide). All of the complexes have been structurally characterized by single-crystal X-ray diffraction analyses and further characterized by infrared spectra (IR), elemental analyses, powder X-ray diffraction (PXRD), and thermogravimetric analyses (TGA). Single crystal X-ray diffraction analysis reveals that complex **1** exhibits a complicated self-catenating three-dimensional (3D) framework that could be decomposed to two interpenetrating (4,6)-coordinated **sun1** nets with point symbol of $\{3\cdot4\cdot6^4\}\{3\cdot4^6\cdot5^2\cdot6^4\cdot7^2\}_2$. Complex **2** is a 2-fold interpenetrating (3,4)-coordinated new topology **sun2** with point symbol of $\{10^3\}_2\{10^6\}_3$. In complex **3**, both the tib and pdac act as a bidentate bridging ligand and extend the tetrahedral Zn(II) centers to an interesting one-dimensional (1D) independent single-wall metal−organic nanotube (SWMONT). Differently, the tib and pdac become tridentate and bidentate linkers in complex **4**, respectively, which extend the Zn(II) centers to the resulting 2-fold interpenetrating (3,4)-coordinated network with a **srd** topology and the point symbol is $\{6^3\}_2\{6^4\cdot9^2\}_3$. Complex **5** is a (3,4)-coordinated self-penetrating network **sun3** with point symbol of $\{10^3\}\{10^6\}$. This net could be further decomposed to two interpenetrating 3-coordinated 10^3 **srs** ($SrSi_2$) subnets by omitting the 2-coordinated pma linker, while complex **6** shows an undulated 2D **3,3L4** layer, which is interdigitated with each other to form a 3D supramoleular framework stabilized by hydrogen bonds. The structural and topological differences of the six CPs indicate that the auxiliary polycarboxylates and solvents play important roles in the formation of the final structures. Furthermore, the thermal stability and photoluminescence properties of the complexes were investigated.

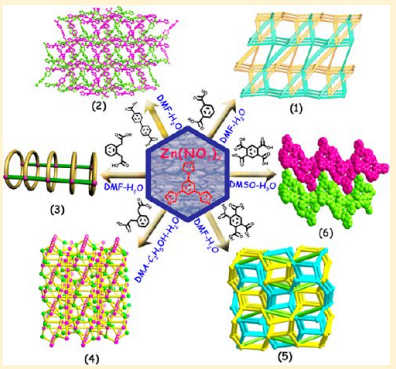

INTRODUCTION

Recently, great attention has been paid to the rapidly growing field of crystal engineering of one-, two-, and three-dimensional (1D, 2D, 3D) coordination polymers (CPs), not only for their structural and topological diversities but also for their potential application as functional materials in catalysis, optics, magnetism, molecular architectures, materials chemistry, etc.[1,2] Despite tremendous progress, it is still a very difficult task to design and predict a new CP structure with a specific net topology.[3,4] The same reactants can usually result in completely different framework structures because of the extreme sensitivity of self-assembly to reaction conditions used, such as solvent, temperature, concentration, and ratio of reactants, reaction time, and pH.[5,6] In this regard, "old" ligands also have chance to find their new niche in the field of crystal engineering. Up to now, the rigid tripodal ligand 1,3,5-tris(1-imidazolyl)benzene (tib) has been justified as an efficient and versatile organic building unit for construction of coordination architectures by Sun and Zheng et al. groups;[7] however, we believe that the CPs of this ligand with varied structures and topologies could still be achieved by changing assembly environments and strategies. Because of the strong coordination affinity and capability of satisfying and mediating the geometric need of metal centers, it is also effective to introduce auxiliary polycarboxylate linkers in preparing mixed ligands CPs with higher-dimensional structures and novel topologies, which have been proven by us as well as many other groups.[8] Hence, systematic research on coordination chemistry of this ligand is deserved for not only

Received: November 26, 2012
Revised: January 5, 2013
Published: February 1, 2013

 © 2013 American Chemical Society dx.doi.org/10.1021/cg3017358 | *Cryst. Growth Des.* 2013, 13, 1277−1289

understanding the control of structure and topology of CPs but also enriching its coordination chemistry.

On the other hand, among the fascinating phenomena contributing much to the topological diversity are the interpenetration and polycatenation between independent motifs, which, as a special way of nature to avoid voids, is frequently encountered in CPs.[9] However, much less common is self-catenation (or self-penetration), a peculiar type of entanglement for which the mutually catenated rings belong to the same net. Although the prediction and design of self-catenation are still a formidable challenge, it has evoked increasing interest recently.[10] Undoubtedly, the exploitation of entangled structures can be helpful not only for both the design and analysis of crystal structures but also for understanding the relationships between the structure and function of these CPs.

On the basis of aforementioned considerations, we consider that the simultaneous employment of tib ligand and aromatic polycarboxylates (Scheme 1) will contribute to the formation of

Scheme 1. Structures of Multidentate N-Donor and Polycarboxylate Ligands Used in This Work

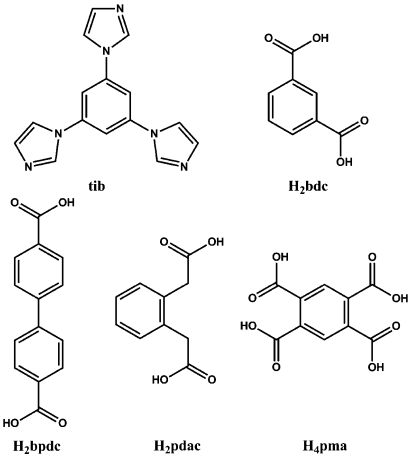

various architectures and help chemists understand the process of self-assembly. Herein, we successfully apply this strategy and obtain six novel CPs, namely, $\{[Zn_8(tib)_5(bdc)_8(H_2O)]\cdot 7DMF\cdot 18H_2O\}_n$ (**1**), $\{[Zn_3(tib)_2(bpdc)_3]\cdot 5H_2O\}_n$ (**2**), $\{[Zn(tib)(pdac)]\cdot 1.5H_2O\}_n$ (**3**) (**3**), $\{[Zn_6(tib)_2(pdac)_3]\cdot DMA\cdot 2H_2O\}_n$ (**4**), $\{[Zn_2(tib)_2(pma)]\cdot 4H_2O\}_n$ (**5**), $\{[Zn_2(tib)(Htib)(H_2pma)(Hpma)]\cdot 2H_2O\}_n$ (**6**) (tib = 1,3,5-tris(1-imidazolyl)benzene H_2bdc = 1,3-benzenedicarboxylic acid, H_2bpdc = 4,4′-biphenyldicarboxylic acid, H_2pdac = 1,2-phenylenediacetic acid, H_4pma = pyromellitic acid, DMF = *N*,*N*′-dimenthylformamide, DMA = *N*,*N*′-dimethylacetamide). Complexes **1** and **5** show novel self-catenating 3D frameworks based on 2-fold interpenetrating (4,6)-coordinated and 3-coordinated 10^3-**srs** subnets, respectively, while **2** and **4** are 2-fold interpenetrating (3,4)-coordinated networks but with different topologies. Complexes **3** and **6** show a 1D metal–organic nanotube and 2D undulated layer, respectively (Scheme 2). Their syntheses, crystal structures, topologies, thermal stabilities, and photoluminescent properties are reported in this paper.

EXPERIMENTAL SECTION

Materials and General Methods. All chemicals and solvents used in the syntheses were analytical grade and used without further purification. C, N, and H analyses were performed on an EA1110

Scheme 2. Synthetic Procedures of Six CPs

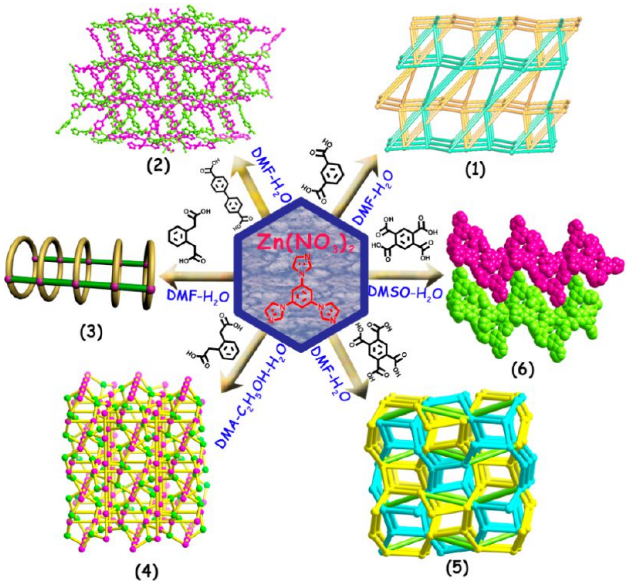

CHNS-0 CE 65 elemental analyzer. IR (KBr pellet) spectra were recorded on a Nicolet Magna750FT-IR spectrometer. Powder X-ray diffraction (PXRD) measurements were recorded on a D/Max-2500 X-ray diffractometer using Cu Kα radiation. The fluorescent spectra were measured on an F-4500 fluorescence spectrophotometer (slit width: 5 nm; sensitivity: high). Thermogravimetric analyses (TGA) were performed on a Netzsch STA 449C thermal analyzer from room temperature to 800 °C under nitrogen atmosphere at a heating rate of 10 °C/min.

Preparation of Complexes 1–6. Preparation of Complexes 1–6. *$\{[Zn_8(tib)_5(bdc)_8(H_2O)]\cdot 7DMF\cdot 18H_2O\}_n$ (1).* A mixture of $Zn(NO_3)_2\cdot 6H_2O$ (16 mg, 0.050 mmol), tib (1.7 mg, 0.006 mmol), H_2bdc (8.4 mg, 0.043 mmol), KOH (0.1 M, 0.05 mL) and 1.0 mL DMF-H_2O (v:v = 1:1) were sealed in a glass tube and heated to 120 °C in 8 h, kept 120 °C for 84 h , and then slowly cooled to 30 °C in 13 h. The pale-yellow crystals were collected, washed with EtOH, and dried in the air (yield: 80%). Elemental analysis calcd (%) for 1 ($C_{160}H_{177}N_{37}O_{58}Zn_8$): C 47.22, H 4.38, N 12.74; found: C 46.89, H 4.61, N 13.27. Selected IR peaks (cm^{-1}): 3432 (s), 1616 (s), 1567 (s), 1494 (s), 1390 (m), 1347 (m), 756 (m) 649 (m).

$\{[Zn_3(tib)_2(bpdc)_3]\cdot 5H_2O\}_n$ (2). A mixture of $Zn(NO_3)_2\cdot 6H_2O$ (16 mg, 0.050 mmol), tib (3 mg, 0.011 mmol), H_2bpdc (5 mg, 0.021 mmol), KOH (0.1 M, 0.05 mL) and 1.0 mL of DMF-H_2O (v:v = 1:1) were sealed in a glass tube and heated to 120 °C in 10 h, kept 120 °C for 84 h, and then slowly cooled to 30 °C in 13 h. The pale-yellow crystals were collected, washed with EtOH, and dried in the air (yield: 80%). Elemental analysis calcd (%) for 2 ($C_{72}H_{58}N_{12}O_{17}Zn_3$): C 55.45, H 3.75, N 10.78; found: C 55.04, H 3.89, N 10.61. Selected IR peaks (cm^{-1}): 3442 (s), 1606 (s), 1345 (s), 1076 (m), 768 (m).

$\{[Zn(tib)(pdac)]\cdot 1.5H_2O\}_n$ (3). A mixture of $Zn(NO_3)_2\cdot 6H_2O$ (16 mg, 0.050 mmol), tib (3 mg, 0.011 mmol), H_2pdac (5 mg, 0.027 mmol), KOH (0.1 M, 0.05 mL), and 1.0 mL of DMF-H_2O (v:v = 1:1) were sealed in a glass tube and heated to 120 °C in 10 h, kept 120 °C for 83 h, and then slowly cooled to 30 °C in 13 h. The pale-yellow crystals were collected, washed with EtOH, and dried in the air (yield: 80%). Elemental analysis calcd (%) for **3** ($C_{25}H_{23}N_6O_{5.5}Zn$): C 53.54, H 4.13, N 14.98; found: C 53.19, H 4.34, N 14.22. Selected IR peaks (cm^{-1}): 3442 (s), 1622 (s), 1509 (s), 1360 (s), 1253 (w), 1073 (m), 1012 (w), 744 (m), 649 (w).

$\{[Zn_6(tib)_2(pdac)_3]\cdot DMA\cdot 2H_2O\}_n$ (4). The synthetic procedure was similar to that of **3**, except that solvent system was changed to 1 mL of DMA-C_2H_5OH-H_2O (v:v:v = 5:2:1). The pale-yellow crystals were collected, washed with EtOH, and dried in the air (yield: 80%). Elemental analysis calcd (%) for **4** ($C_{124}H_{109}N_{25}O_{27}Zn_6$): C 53.69, H 3.96, N 12.62; found: C 53.02, H 4.23, N 12.40. Selected IR peaks

dx.doi.org/10.1021/cg3017358 | Cryst. Growth Des. 2013, 13, 1277–1289

Table 1. Crystal Data for 1−4[a]

compound	1	2	3	4	5	6
empirical formula	$C_{139}H_{92}N_{30}O_{33}Zn_8$	$C_{24}H_{16}N_4O_4Zn$	$C_{25}H_{23}N_6O_{5.5}Zn$	$C_{124}H_{109}N_{25}O_{27}Zn_6$	$C_{20}H_{17}N_6O_6Zn$	$C_{50}H_{36}N_{12}O_{18}Zn_2$
formula weight	3233.39	489.78	560.88	2773.68	502.77	1223.65
temperature/K	298(2)	298(2)	298(2)	298(2)	298(2)	298(2)
crystal system	triclinic	trigonal	monoclinic	cubic	orthorhombic	triclinic
space group	$P\bar{1}$	$P\bar{3}$	$P2_1/c$	$Fd\bar{3}c$	$Pbca$	$P\bar{1}$
a/Å	17.9946(19)	19.0758(19)	8.5692(12)	36.3142(19)	14.705(2)	7.7103(6)
b/Å	20.490(2)	19.0758(19)	20.821(3)	36.3142(19)	15.934(3)	17.4489(13)
c/Å	27.772(3)	11.429(2)	15.037(2)	36.3142(19)	16.796(3)	18.0994(13)
α/°	82.113(2)	90.00	90.00	90.00	90.00	85.9990(10)
β/°	72.543(2)	90.00	97.053(2)	90.00	90.00	89.1120(10)
γ/°	84.884(2)	120.00	90.00	90.00	90.00	83.6500(10)
volume/Å^3	9663.3(18)	3601.6(9)	2662.6(6)	47888(4)	3935.6(11)	2414.1(3)
Z	2	6	4	16	8	2
ρ_{calc} mg/mm^3	1.111	1.355	1.392	1.470	1.697	1.683
μ/mm^{-1}	1.039	1.059	0.970	1.265	1.304	1.088
F(000)	3280.0	1500.0	1144.0	21696.0	2056.0	1248.0
2Θ range for data collection	2 to 50°	3.56 to 49.98°	4.78 to 50°	3.18 to 49.98°	4.48 to 50°	3.14 to 50°
reflections collected	48128	17216	13112	35929	13404	12041
independent reflections	33613[R(int) = 0.0564]	4132[R(int) = 0.0470]	4683[R(int) = 0.0249]	1754[R(int) = 0.1050]	3462[R(int) = 0.0685]	8409[R(int) = 0.0155]
data/restraints/parameters	33613/0/1861	4132/168/460	4683/0/343	1754/25/132	3462/0/298	8409/6/767
goodness-of-fit on F^2	0.934	1.084	1.072	1.094	1.020	1.028
final R indexes [$I \geq 2\sigma(I)$]	R_1 = 0.0701, wR_2 = 0.1630	R_1 = 0.0894, wR_2 = 0.2307	R_1 = 0.0441, wR_2 = 0.1281	R_1 = 0.0627, wR_2 = 0.1725	R_1 = 0.0520, wR_2 = 0.1365	R_1 = 0.0329, wR_2 = 0.0870
final R indexes [all data]	R_1 = 0.1497, wR_2 = 0.1791	R_1 = 0.0980, wR_2 = 0.2354	R_1 = 0.0553, wR_2 = 0.1371	R_1 = 0.0972, wR_2 = 0.1867	R_1 = 0.0781, wR_2 = 0.1555	R_1 = 0.0407, wR_2 = 0.0920
largest diff peak/hole/e Å^{-3}	0.72/−0.71	1.11/−0.94	0.85/−0.65	0.49/−0.51	1.00/−0.93	0.51/−0.38

[a] $R_1 = \Sigma||F_o| - |F_c||/\Sigma|F_o|$, $wR_2 = [\Sigma w(F_o^2 - F_c^2)^2]/\Sigma w(F_o^2)^2]^{1/2}$.

(cm^{-1}): 3442 (s), 1613 (s), 1512 (s), 1381 (m), 1356 (m), 1256 (w), 1079 (w), 646 (m).

{[Zn_2(tib)$_2$(pma)]·4H_2O}$_n$ (**5**). A mixture of $Zn(NO_3)_2$·6H_2O (16 mg, 0.050 mmol), tib (3 mg, 0.011 mmol), H_2pma (6 mg, 0.027 mmol), KOH (0.1 M, 0.05 mL), and 1.0 mL of DMF-H_2O (v:v = 1:1) were sealed in a glass tube, heated to 120 °C in 8 h, kept 120 °C for 83 h, and then slowly cooled to 30 °C in 13 h. The pale-yellow crystals were collected, washed with EtOH, and dried in the air (yield: 80%). Elemental analysis calcd (%) for **5** ($C_{20}H_{17}N_6O_6Zn$): C 47.78, H 3.41, N 16.72; found: C 47.92, H 3.68, N 16.44. Selected IR peaks (cm^{-1}): 3439 (s), 1622 (s), 1518 (s), 1359 (m), 1320 (m), 1262 (m), 1079 (w), 1012 (w), 756 (w), 643 (w).

{[Zn_2(tib)(Htib)(H_2pma)(Hpma)]·2H_2O}$_n$ (**6**). The synthetic procedure was similar to that of **3**, except that solvent system was changed to 1.0 mL of DMSO-H_2O (v:v = 1:1). The pale-yellow crystals were collected, washed with EtOH, and dried in the air (yield: 80%). Elemental analysis calcd (%) for **6** ($C_{50}H_{36}N_{12}O_{18}Zn_2$): C 49.08, H 2.97, N 13.74; found: C 49.34, H 2.62, N 13.88. Selected IR peaks (cm^{-1}): 3436 (s), 1707 (m), 1622 (s), 1515 (s), 1344 (s), 1076 (w), 1015 (w), 646 (w).

X-ray Crystallography. Single crystals of the complexes **1**−**6** with appropriate dimensions were chosen under an optical microscope and quickly coated with high vacuum grease (Dow Corning Corporation) before being mounted on a glass fiber for data collection. Data for them were collected on a Bruker Apex II CCD diffractometer with graphite-monochromated Mo Kα radiation source (λ = 0.71073 Å). A preliminary orientation matrix and unit cell parameters were determined from 3 runs of 12 frames each; each frame corresponds to a 0.5° scan in 5 s, followed by spot integration and least-squares refinement. For **1**−**6**, data were measured using ω scans of 0.5° per frame for 10 s until a complete hemisphere had been collected. Cell parameters were retrieved using SMART software and refined with SAINT on all observed reflections.[11] Data reduction was performed with the SAINT software and corrected for Lorentz and polarization effects. Absorption corrections were applied with the program SADABS.[11] In all cases, the highest possible space group was chosen. All structures were solved by direct methods using SHELXS-97[12] and refined on F^2 by full-matrix least-squares procedures with SHELXL-97.[13] Atoms were located from iterative examination of difference F-maps following least-squares refinements of the earlier models. Hydrogen atoms were placed in calculated positions and included as riding atoms with isotropic displacement parameters 1.2−1.5 times U_{eq} of the attached C atoms. There are some solvent accessible void volumes in the crystals of **1**, **2**, **4**, which are occupied by highly disordered water molecules. No satisfactory disorder model could be achieved, and therefore the SQUEEZE program implemented in PLATON[14] was used to remove these electron densities. The solvents for **1**, **2**, **4** are tentatively assigned based on TGA, elemental analysis as well as the SQUEEZE results. To assist in the refinement of **2**, **4**, and **6**, several restraints were applied: (1) some C−C bonds restrained to be similar, and some atoms restrained to be coplanar (DFIX and FLAT); (2) thermal parameters on adjacent atoms in disordered moieties were restrained to be similar (SIMU and ISOR). All structures were examined using the Addsym subroutine of PLATON to ensure that no additional symmetry could be applied to the models. Pertinent crystallographic data collection and refinement parameters are collated in Table 1. Selected bond lengths and angles are collated in Table 2. Topological analysis of coordination networks in all complexes was performed with the program package TOPOS.[15]

RESULTS AND DISCUSSION

Synthesis and General Characterization. The synthesis for the target six complexes were performed in seal glass tube (2 mL) by utilizing the solvothermal method with the different stoichiometric ratio for the starting materials in the presence of

dx.doi.org/10.1021/cg3017358 | Cryst. Growth Des. 2013, 13, 1277−1289

Table 2. Selected Bond Lengths (Å) and Angles (°) for 1−6

				Complex **1**[a]			
Zn1—O16^{i}	1.936 (4)	Zn2—O1	1.947 (5)	Zn3—O4	1.903 (5)	Zn4—O14	1.936 (4)
Zn1—O23	1.942 (6)	Zn2—N25	1.984 (6)	Zn3—O27^{ii}	1.939 (5)	Zn4—O9	1.991 (5)
Zn1—N13	1.985 (6)	Zn2—O5	2.042 (5)	Zn3—N16^{iii}	1.984 (7)	Zn4—N22^{v}	2.014 (5)
Zn1—N19	1.999 (5)	Zn2—N24	2.051 (5)	Zn3—N4^{iv}	1.998 (6)	Zn4—N28	2.017 (5)
Zn5—O12	1.954 (5)	Zn6—O21	1.917 (6)	Zn7—O7^{ix}	1.907 (7)	Zn8—O25	1.932 (4)
Zn5—O19^{vi}	1.967 (6)	Zn6—N7	1.972 (6)	Zn7—O29^{viii}	1.951 (5)	Zn8—O31	1.967 (5)
Zn5—N30^{v}	2.015 (6)	Zn6—O17	2.014 (5)	Zn7—N9	1.985 (6)	Zn8—N1	1.989 (5)
Zn5—N17^{vii}	2.108 (17)	Zn6—N6^{viii}	2.038 (6)	Zn7—O1W	2.045 (7)	Zn8—N11	2.010 (5)
O16^{i}—Zn1—O23	111.0 (2)	O1—Zn2—N25	118.6 (3)	O4—Zn3—O27^{ii}	112.3 (2)	O14—Zn4—O9	106.7 (2)
O16^{i}—Zn1—N13	112.6 (3)	O1—Zn2—O5	114.3 (2)	O4—Zn3—N16^{iii}	109.8 (3)	O14—Zn4—N22^{v}	99.3 (2)
O23—Zn1—N13	111.7 (3)	N25—Zn2—O5	106.9 (2)	O27^{ii}—Zn3—N16^{iii}	111.9 (2)	O9—Zn4—N22^{v}	109.61 (19)
O16^{i}—Zn1—N19	99.3 (2)	O1—Zn2—N24	102.2 (2)	O4—Zn3—N4^{iv}	119.5 (2)	O14—Zn4—N28	111.9 (2)
O23—Zn1—N19	116.7 (2)	N25—Zn2—N24	112.2 (2)	O27^{ii}—Zn3—N4^{iv}	97.8 (2)	O9—Zn4—N28	109.2 (2)
N13—Zn1—N19	104.9 (3)	O5—Zn2—N24	101.3 (3)	N16^{iii}—Zn3—N4^{iv}	104.9 (2)	N22^{v}—Zn4—N28	119.2 (2)
O12—Zn5—O19^{vi}	109.9 (2)	O21—Zn6—N7	121.6 (3)	O7^{ix}—Zn7—O29^{viii}	107.9 (3)	O25—Zn8—O31	106.3 (2)
O19^{vi}—Zn5—N30^{v}	116.9 (2)	O21—Zn6—O17	110.0 (3)	O7^{ix}—Zn7—N9	118.4 (3)	O25—Zn8—N1	99.0 (2)
O12—Zn5—N17^{vii}	107.6 (5)	N7—Zn6—O17	110.8 (2)	O29^{viii}—Zn7—N9	103.6 (3)	O31—Zn8—N1	108.0 (2)
O12—Zn5—N30^{v}	101.5 (2)	O21—Zn6—N6^{viii}	102.3 (3)	O7^{ix}—Zn7—O1W	101.4 (3)	O25—Zn8—N11	114.1 (2)
O19^{vi}—Zn5—N17^{vii}	111.4 (5)	N7—Zn6—N6^{viii}	110.7 (3)	O29^{viii}—Zn7—O1W	115.1 (3)	O31—Zn8—N11	110.9 (2)
N30^{v}—Zn5—N17^{vii}	108.8 (5)	O17—Zn6—N6^{viii}	98.7 (3)	N9—Zn7—O1W	110.9 (3)	N1—Zn8—N11	117.4 (2)
				Complex **2**[b]			
Zn1—O1	1.921 (13)	Zn1—N1	1.996 (6)	Zn1—O4^{i}	1.936 (6)	Zn1—N3	2.095 (18)
O1—Zn1—O4^{i}	95.9 (5)	O1—Zn1—N3	109.9 (7)	O1—Zn1—N1	124.6 (5)	O4^{i}—Zn1—N3	123.5 (5)
O4^{i}—Zn1—N1	107.9 (3)	N1—Zn1—N3	97.4 (5)				
				Complex **3**[c]			
Zn1—O1	1.933 (2)	Zn1—N1	1.995 (3)	Zn1—O4^{i}	1.944 (3)	Zn1—N3^{ii}	2.021 (3)
O1—Zn1—O4^{i}	107.85(11)	O1—Zn1—N3^{ii}	94.88(10)	O4^{i}—Zn1—N1	111.05(11)	N1—Zn1—N3^{ii}	113.61(11)
O1—Zn1—N1	116.80(11)	O4^{i}—Zn1—N3^{ii}	111.64(11)				
				Complex **4**[d]			
Zn1—O1	1.946 (5)	Zn1—N1	2.020 (5)				
O1^{i}—Zn1—N1^{i}	101.2 (2)	O1^{i}—Zn1—O1	112.2 (4)	O1—Zn1—N1^{i}	119.45 (19)	N1^{i}—Zn1—N1	104.1 (3)
				Complex **5**[e]			
Zn1—O1	1.911 (3)	Zn1—N1	2.010 (4)	Zn1—N4^{i}	1.985 (4)	Zn1—N6^{ii}	2.024 (4)
O1—Zn1—N4^{i}	112.85 (16)	O1—Zn1—N6^{ii}	97.59 (16)	N4^{i}—Zn1—N1	112.99 (16)	N1—Zn1—N6^{ii}	100.13 (16)
O1—Zn1—N1	116.09 (16)	N4^{i}—Zn1—N6^{ii}	115.70 (16)				
				Complex **6**[f]			
Zn1—O3^{i}	1.9087 (18)	Zn1—O1	1.961 (2)	Zn1—N7	1.993 (2)	Zn1—N1	1.996 (2)
Zn2—N12	1.994 (2)	Zn2—N4^{ii}	2.013 (2)	Zn2—O9	1.9653 (18)	Zn2—N10^{iii}	2.025 (2)
O3^{i}—Zn1—O1	105.12 (10)	O3^{i}—Zn1—N1	130.23 (9)	O9—Zn2—N12	114.12 (8)	O9—Zn2—N10^{iii}	100.62 (8)
O3^{i}—Zn1—N7	101.52 (9)	O1—Zn1—N1	96.43 (9)	O9—Zn2—N4^{ii}	113.31 (9)	N12—Zn2—N10^{iii}	111.53 (8)
O1—Zn1—N7	116.36 (8)	N7—Zn1—N1	108.10 (8)	N12—Zn2—N4^{ii}	110.05 (9)	N4^{ii}—Zn2—N10^{iii}	106.64 (9)

[a]Symmetry codes: (i) $x + 1, y + 1, z$; (ii) $x, y, z + 1$; (iii) $-x + 2, -y + 2, -z + 3$; (iv) $x, y - 1, z + 1$; (v) $x - 1, y, z$; (vi) $x - 1, y - 1, z$; (vii) $-x + 1, -y + 2, -z + 2$; (viii) $x + 1, y, z$; (ix) $x + 1, y, z - 1$. [b]Symmetry code: (i) $-x + y + 1, -x + 1, z + 1$. [c]Symmetry codes: (i) $x + 1, y, z$; (ii) $-x + 1, -y + 1, -z$. [d]Symmetry code: (i) $-x + 1/2, -z + 1/2, -y + 1/2$. [e]Symmetry codes: (i) $x - 1/2, -y + 1/2, -z + 1$; (ii) $-x + 2, y - 1/2, -z + 3/2$. [f]Symmetry codes: (i) $-x + 2, -y, -z + 1$; (ii) $-x + 1, -y, -z$; (iii) $-x, -y, -z$.

KOH. As a consideration for the safety in the lab, the reaction temperature was kept to no higher than 120 °C. The one-pot mixture was heated to an appropriate temperature and held for 48−72 h and then cooled at a descent rate of 10 °C/h. Finally, the crystals suitable for single-crystal X-ray diffraction analysis were obtained after cooling to room temperature. All the complexes **1**−**6** are stable in the solid state upon extended exposure to air. They have poor solubility in common organic solvents and only are slightly soluble in very high polarity solvents, such as DMF, DEF, and DMSO.

PXRD has been used to check the phase purity of the bulk samples in the solid state. For complexes **1**−**6**, the measured PXRD patterns closely match the simulated patterns generated from the results of single-crystal diffraction data (Figure S1, Supporting Information), indicative of pure products. In their IR spectra (Figure S2−S8, Supporting Information), the absorption bands resulting from the skeletal vibrations of the aromatic ring were observed in the 1400−1600 cm^{-1} region. The ν_{as}(COO), ν_{s}(COO) bands appear at 1616, 1390 cm^{-1}; 1606, 1345 cm^{-1}; 1622, 1360 cm^{-1}, 1613, 1381 cm^{-1}, 1622, 1359 cm^{-1} and 1622, 1344 cm^{-1} for **1**−**6**. The $\Delta\nu$ values [$\Delta\nu = \nu_{as}(COO) - \nu_{s}(COO)$] are 220 cm^{-1} for **1**, 261 cm^{-1} for **2**, 262 cm^{-1} for **3**, 232 cm^{-1} for **4**, 263 cm^{-1} for 5, and 278 cm^{-1} for **6**, respectively, in good agreement with their monodentate coordination mode of the carboxylate groups.[16] Broad peaks at around 3440 cm^{-1} for the spectra of **1**−**6** can be attributed to

dx.doi.org/10.1021/cg3017358 | Cryst. Growth Des. 2013, 13, 1277−1289

the O−H stretch of lattice or coordinated water molecules. These results are also confirmed by single-crystal structure analysis.

Structure Descriptions. *{[$Zn_8(tib)_5(bdc)_8(H_2O)$]·7DMF·18H_2O}$_n$ (1).* X-ray single-crystal diffraction analysis reveals that **1** is a 3D network. It crystallizes in the triclinic crystal system with space group of $P\bar{1}$. The asymmetric unit contains eight crystallographically independent Zn(II) ion, five tib ligand, eight bdc dianions, one coordinated water molecule and lattice solvents molecules. As shown in Figure 1, each Zn

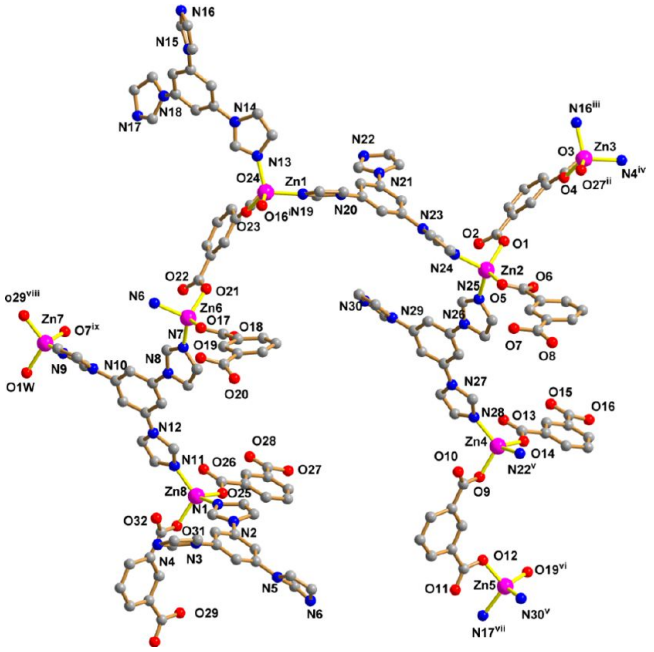

Figure 1. The coordination environment of Zn(II) ion in **1**. (Symmetry codes: (i) $x + 1, y + 1, z$; (ii) $x, y, z + 1$; (iii) $-x + 2, -y + 2, -z + 3$; (iv) $x, y - 1, z + 1$; (v) $x - 1, y, z$; (vi) $x - 1, y - 1, z$; (vii) $-x + 1, -y + 2, -z + 2$; (viii) $x + 1, y, z$; (ix) $x + 1, y, z - 1$.)

atom locates in a ZnN_2O_2 tetrahedral geometry. The average bond lengths around Zn1−Zn8 are 1.966(5), 2.006(5), 1.956(5), 1.990(5), 2.011(5), 1.985(5), 1.948(5), and 1.975(5) Å, respectively. The distortion of the tetrahedron can be indicated by the calculated value of the τ_4 parameter introduced by Houser[17] to describe the geometry of a four-coordinate metal system, which are 0.92, 0.90, 0.91, 0.92, 0.94, 0.90, 0.91, and 0.91 for Zn1−Zn8, respectively (for ideal tetrahedron $\tau_4 = 1$). Both Zn−N and Zn−O bond lengths are well-matched to those observed in similar complexes.[18] The tib and bdc ligands adopt a tri- and bidentate bridging mode to extend the Zn(II) atoms to the resulting complicated 3D network (Figure 2a). Calculations using PLATON show that the voids in complex **1** occupy 37.5% of the crystal volume (after the removal of the guest molecules).

Better insight of the complicated 3D architecture can be achieved by topology analysis. This 3D net shows an interesting self-catenation phenomenon (Figure 2b), but most important is that it can be easily decomposed to two interpenetrating 3D nets by breaking just two Zn1−N bonds. Each of the decomposed 3D nets is not self-catenating, so the complex self-catenation in the initial net is completely described by interpenetration. This decomposition can be easily found with the TOPOS cluster simplification procedure.[19] This procedure

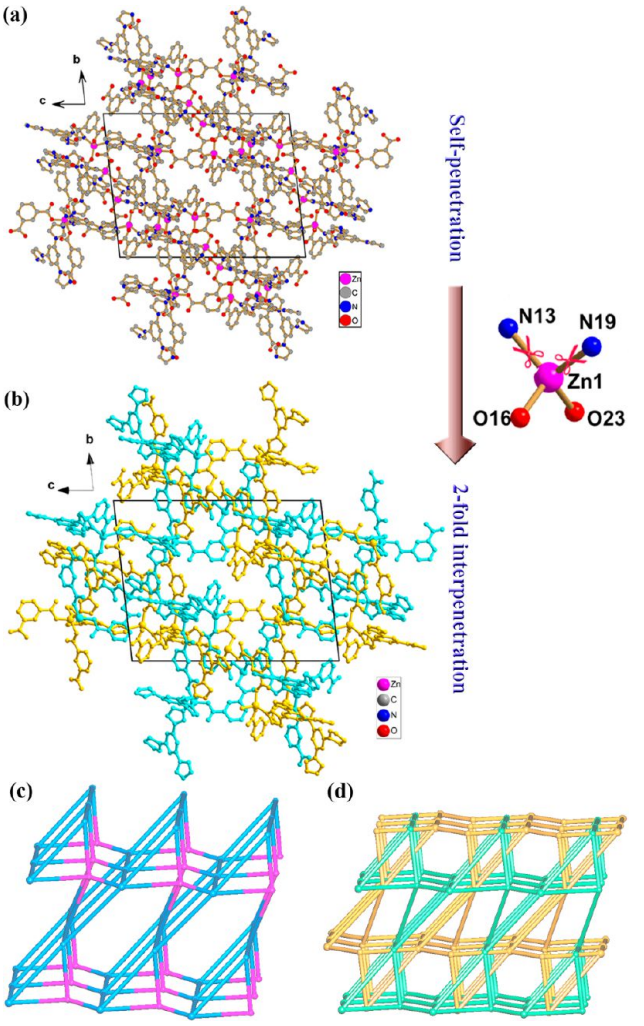

Figure 2. (a) Ball-and-stick view of self-penetrating 3D framework. (b) 2-fold interpenetrating network formed by breaking two Zn1−N bonds highlighted by red dashed lines. (c) Simplified (4,6)-coordinated single net. (d) Simplified 2-fold interpenetrating network.

splits the coordination network into topologically distinct molecular or polymeric cluster groups. Each of the decomposed nets can be described in the cluster representation as 4,6-coordinated net with point symbol of $\{3{\cdot}4{\cdot}6^4\}\{3{\cdot}4^6{\cdot}5^2{\cdot}6^4{\cdot}7^2\}_2$ (Figure 2c,d). This simplified net defines a new topology that is unobserved not only in MOFs, but also unenumerated in the electronic databases EPINET, RCSR, and TOPOS TTD.[20] We have deposited it to the TOPOS TTD Collection under the name **sun1**. Recently a stringent nomenclature has been proposed for interpenetration classification,[21] where the most important distinctions are made between structures containing nets related by displacement vectors only (Class **I**, the most common), those where the nets are symmetry-related (Class **II**) and those that are related by both symmetry and displacement vectors (Class **III**). In **1**, the interpenetration can be classified as type Class **IIa**, $Z = 2$, which means that two identical interpenetrated nets are generated by means of space group interpenetration symmetry element, here is the inversion center, and no interpenetrating translations are allowed in this kind of interpenetration.

Previously, Sun's group used $ZnCl_2$ or $Zn(NO_3)_2{\cdot}6H_2O$ with the same mixed ligands to assemble two CPs with the formulas of $\{[Zn(tib)(bdc)]{\cdot}H_2O\}_n$ and $\{[Zn_2(tib)$-

dx.doi.org/10.1021/cg3017358 | Cryst. Growth Des. 2013, 13, 1277−1289

$(bdc)_2(H_2O)]\cdot 2H_2O\}_n$, respectively.[22] The two CPs range from a neutral 2D rectangular grid network with 4^4-**sql** topology to a 3D (3,4)-coordinated net with $(8^3)_2(8^6)$ topology; these topologies are modulated by counteranions, even though the anions are not included in the resulting structures. On the basis of the structural analysis, the complex **1** in this work is completely different from the above two CPs and also much more complicated than them. Comparing results indicates that the reactant ratios, solvent, temperature, or reaction vessel may strongly influence the resulting structures, which also suggests that the design and prediction of CP structures are still very difficult, even if the same reactants are used.

$\{[Zn_3(tib)_2(bpdc)_3]\cdot 5H_2O\}_n$ ***(2)***. Structural analysis indicates that complex **2** crystallizes in the trigonal $P\bar{3}$ space group. The asymmetric unit of **2** is composed of one crystallographically independent Zn(II) atom, two tib ligands passed by 3-fold axis, one bpdc ligand and highly disordered water molecules. The coordination environment around the Zn(II) atom is exhibited in Figure 3a along with the atom numbering scheme. The Zn1

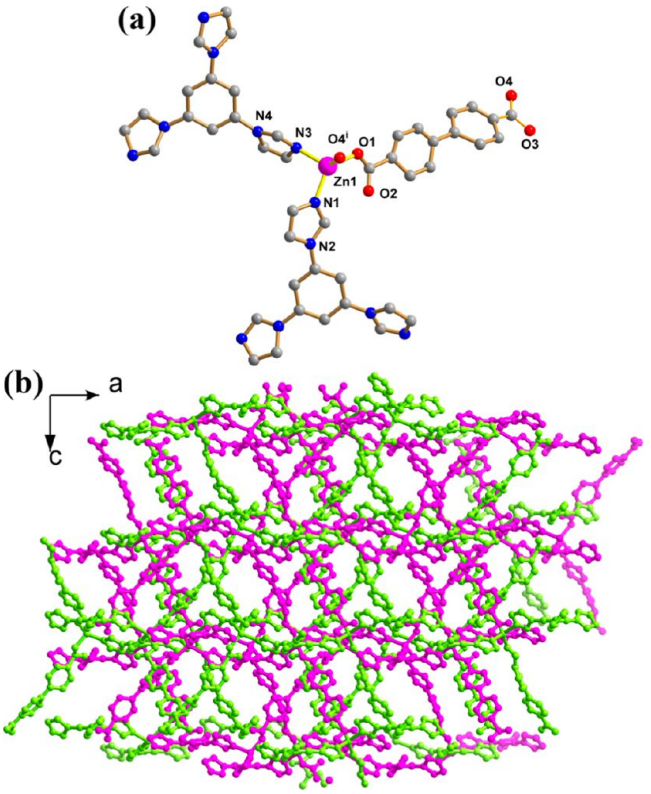

Figure 3. (a) The coordination environment of Zn(II) ions in **2**. (b) The 2-fold interpenetrating 3D network. (Symmetry codes: (i) $-x + y + 1, -x + 1, z + 1$.)

is located in a slightly ZnN_2O_2 tetrahedral geometry ($\tau_4 = 0.77$) completed by two N atoms belonging to two tib ligands and two O atoms from two bpdc ligand. The Zn−N/O bond lengths span the range of 1.921(13)−2.095(18) Å. Each tib ligand coordinates to three Zn(II) atoms with a nonplanar geometry with dihedral angles of ca. 38 and 47°, respectively. On the other hand, the bpdc ligand is a bidentate bridging ligand since each carboxylate group adopts a (κ^1)-μ_1 monodentate coordination mode to connect one Zn(II) atom. Such coordination modes make complex **2** a 2-fold interpenetrating 3D network (Figure 3b).

From a topological point of view, the resulting 3D interpenetrating net relies on the combination of triangle tib and tetrahedral Zn(II) building unit, serving as 3- and 4-coordinated nodes, respectively (Figure 4a,b). As linear bpdc

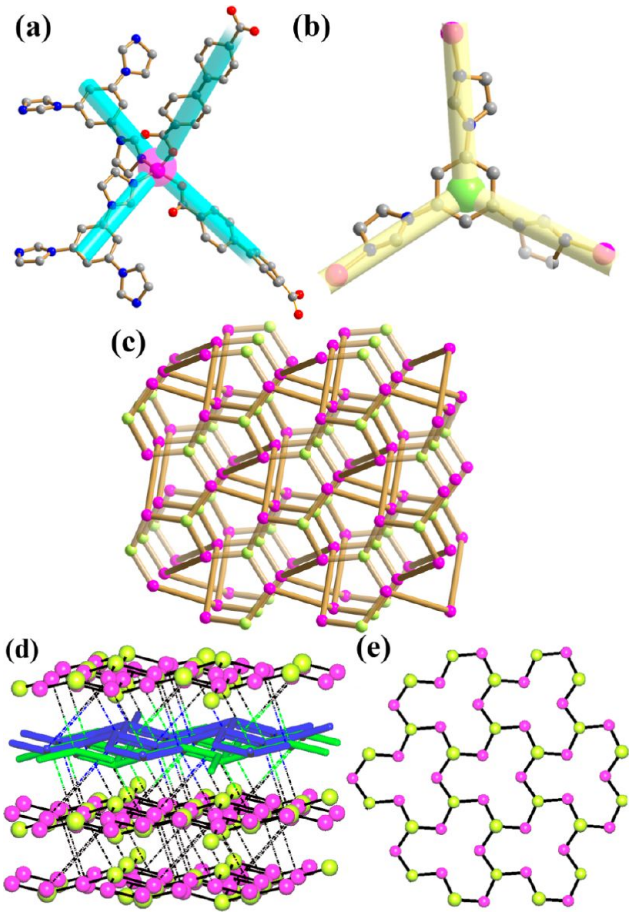

Figure 4. (a) The 4-coordinated tetrahedral Zn(II) building unit in **2**. (b) The 3-coordinated triangle tib node in **2**. (c) Ball-and-stick and schematic representations of simplified 3D 3,4-coordinated net with $\{10^3\}_2\{10^6\}_3$ topology. (d) Representation as a stacking of **hcb** double layers; the dashed lines correspond to bpdc ligands. (e) A single layer in the stacking; the **hcb** topology becomes obvious if one considers tib-Zn-tib links as edges of the simplified net.

only coordinates to two Zn(II) atoms, the network can be simplified as a new binodal 3,4-coordinated net with point symbol of $\{10^3\}_2\{10^6\}_3$ (Figure 4c). We have deposited it to the TOPOS TTD Collection under the name **sun2**. The TOPOS cluster analysis shows that considering only the $Zn_3(tib)_2$ subnets, i.e., ignoring Zn−bpdc contacts, one can represent the coordination polymer as a stacking of doubled honeycomb-like (**hcb**) (001) layers (Figure 4d,e). As a consequence of Mother Nature's horror vacui, two equivalent nets adopt 2-fold interpenetration to minimize the large voids in the single net. However, in spite of interpenetration, **2** still possesses free void space estimated to be about 208.0 $Å^3$, that is, 5.8% of the unit cell. An analysis of the topology of interpenetration reveals that **2** also belongs to Class **II**a; that is, two interpenetrated nets are generated only by symmetry element (here is inversion center) from the single net.

$\{[Zn(tib)(pdac)]\cdot 1.5H_2O\}_n$ ***(3)***. X-ray single-crystal diffraction analysis reveals that **3** is an independent 1D single-wall metal−organic nanotube (SWMONT). It crystallizes in the monoclinic

dx.doi.org/10.1021/cg3017358 | *Cryst. Growth Des.* 2013, 13, 1277−1289

crystal system with space group of $P2_1/c$. The asymmetric unit consists of one Zn(II) ion, one tib ligand, one pdac dianion, and two uncoordinated water molecule. As depicted in Figure 5a, Zn1 is four-coordinated by two nitrogen atoms from two tib

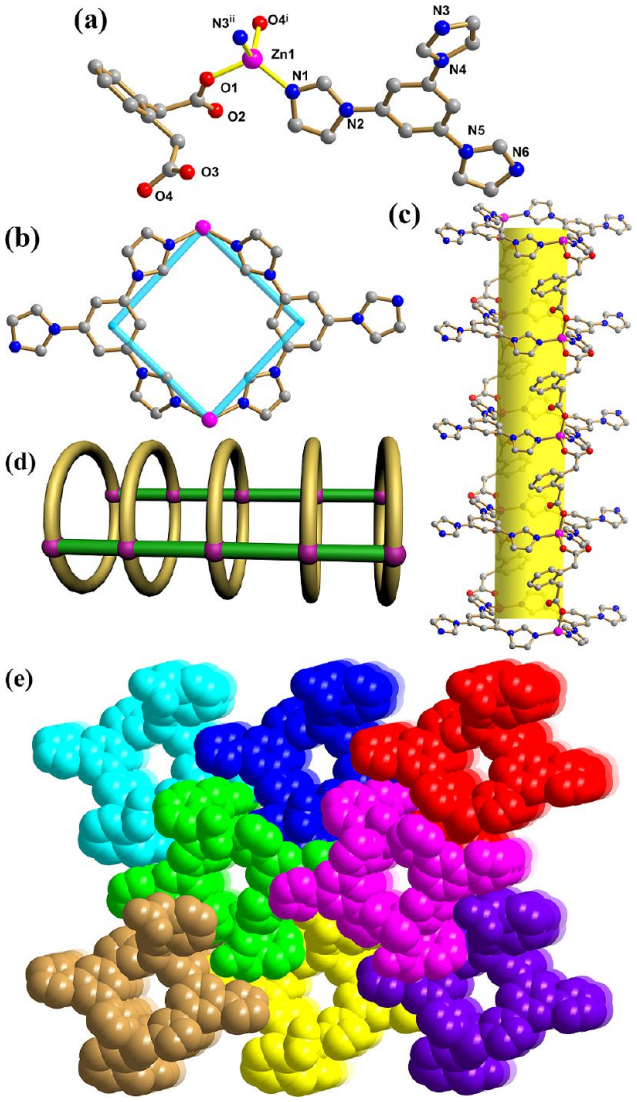

Figure 5. (a) The coordination environment of Zn(II) ion in **3**. (Symmetry codes: (i) $x + 1, y, z$; (ii) $-x + 1, -y + 1, -z$.) (b) Rectangular $[Zn_2(tib)_2]$ metallamacrocycle. (c) Ball-and-stick representations of 1D SWMONT. (d) Schematic representations of simplified 1D SWMONT (purple ball: Zn; green bar: pdac dianion; yellow arc: tib). (e) Packing array of the nanotubes (nanotubes individually colored).

ligand (Zn1−N1 = 1.995(3) and Zn1−N3^{ii} = 2.021(3) Å) and two oxygen atoms from two carboxylate groups of two pdac anions (Zn1−O4^{i} = 1.944(3) and Zn1−O1 = 1.933(2) Å) in a distorted tetrahedral coordination environment ($\tau_4 = 0.90$). It is noteworthy that the tib ligand coordinates with two, rather than three like in **1** and **2**, Zn(II) atoms using two of its three imidazole groups, and the third one with N6 did not participate in the coordination, which has been observed previously.[23] Three dihedral angles formed between the central phenyl ring and three terminal imidazole groups are 23.11(14), 34.67(13), and 13.47(17)°, respectively. (Symmetry codes: (i) $x + 1, y, z$; (ii) $-x + 1, -y + 1, -z$.)

The tib ligand acts as bidentate bridging ligand to bind two Zn(II) atoms to form an approximately rectangular $[Zn_2(tib)_2]$ metallamacrocycle (Figure 5b) with two supplementary interior angles of 91.88 and 88.12°, respectively. Two carboxylate groups of pdac are arranged in the opposite sites relative to the central phenyl ring, giving an *anti* conformation, which link the $[Zn_2(tib)_2]$ metallamacrocycles from the four vertexes to generate an open-ended, hollow SWMONT (Figure 5c) with the interior cross section size of ca. 5.48 × 5.32 Å. In the interior of the SWMONT, two water molecules are hydrogen bonded to form a 1D water chain, and no obvious hydrogen bonding is found between the interior wall of SWMONT and water chain. To illustrate the unique structure of **3**, each Zn center, which is connected to two tib and two pdac ligands, is represented by a distorted tetrahedral four-coordinated node, and the tib and pdac linkers are simplified to angular and linear bars, respectively (Figure 5d). The neighboring SWMONTs are all held together by weak $\pi\cdots\pi$ stacking interaction (3.9273(18) Å) between imidazole and phenyl ring of tib and nonclassical C−H···O to form a 3D supramolecular framework (Figure 5e).

As we know, a few metal−organic nanotubes (MONTs) have been recently reported in the literature.[24] For example, Hong and co-workers synthesized a Cd(II) MONT based on mixed diphenic acid, isonicotinic acid, and 1,2-di(4-pyridyl)ethylene, and a silver nanotube constructed from a flexible tripodal ligand.[25] Zur Loye's group synthesized a 3D framework based on a 3-amino-1,2,4-triazole ligand containing 1D MONT.[26] Lu and co-workers reported a unique type of MOF $[\{[Cd(apab)_2(H_2O)]_3(MOH)\cdot G\}_n]$ (M = Cs^+, K^+, Na^+, apab = 4-amiono-3-[(pyridin-4-ylmethylene)amino]benzoate) consisting of a large SWMONT $[Cd(apab)_2(H_2O)]_{3n}$ with a exterior wall diameter and an interior channel diameter up to 3.2 and 1.4 nm, respectively.[27] However, the above-mentioned MONTs were usually connected via other ligands to form the high-dimensional network.[28] The independent or isolated 1D MONTs are quite scarce and many groups are pursuing this field.[29] For example, our group reported an interesting 1D MONT $[Zn(ATIBDC)(bpy)]\cdot 3H_2O$ (bpy = 4,4′-bipyridine, H_2ATIBDC = 5-amino-2,4,6-triiodoisophthalic acid) in which the Zn(II) ion is first connected by bpy ligands to generate a $[Zn_4(bpy)_4]$ square as the subunit, and then, the ATIBDC links the squares from the four vertexes to generate a 1D MONT.[29k] Dong and co-worker reported a Ag(I) CP in which the Ag(I) ion acts as square planar 4-coordinated nodes, and the angular tetradentate ligands connect the Ag(I) ions to generate a 1D MONT.[30] Sun's group synthesized a Zn complex 1D MONT with tri(imidazole) flexible ligand.[31] Dyson and co-workers synthesized a novel Zn(II) MONT with a imidazolediacatatic ligand.[32] Cheng and co-workers reported a bimetallic 1D MONT $\{Mn(H_2O)_2[Ru(bipy)(CN)_4]\}$ (bipy = 2,2′-bipyridine).[33] Du and co-workers synthesized a 1D nanotube $[Cu(SCN)(bpp)](DMF)_{0.5}$ with CuSCN and flexible 1,3-bis(pyridin-4-yl)propane (bpp) ligand.[29g]

*$\{[Zn_6(tib)_2(pdac)_3]\cdot DMA\cdot 2H_2O\}_n$ (**4**).* When the solvent system in the synthesis of **3** was changed from DMF-H_2O (v:v = 1:1) to DMA-C_2H_5OH-H_2O (v:v:v = 5:2:1), complex **4** was obtained as a 2-fold interpenetrated 3,4-coordinated 3D network like **2** but with a **srd** topology. It crystallized in cubic space group $Fd\bar{3}c$ with very high symmetry. The asymmetric unit of **4** consists of half of the Zn(II) center, one-third of the tib ligand, and half of pdac dianion; other disordered guest molecules are not crystallographically well-defined. Analysis of the local symmetry of the metal cation and ligand showed that

dx.doi.org/10.1021/cg3017358 | *Cryst. Growth Des.* 2013, 13, 1277−1289

the Zn(II) center was passed by 2-fold axis (site occupancy factor (SOF) = 0.5), and another 2-fold axis of rotation passing through the midponits of C10−C10 and C8−C8 bisected the pdac dianion, the tib resides on the other special symmetry site containing a 3-fold axis. As depicted in Figure 6a, the Zn(II) center is bound to two imidazole nitrogen atoms and two carboxylate oxygen atoms (Zn1−O1 = 1.946(5); Zn1−N1 = 2.020(5) Å) in a tetrahedral manner (τ_4 = 0.84). The tib ligand coordinates to three Zn(II) atoms with a nonplanar geometry with dihedral angles of 25.4(3)°. On the other hand, the pdac ligand with an *anti* conformation to adopts a (κ^1)-(κ^1)-μ_2 bidentate coordination mode to connect the Zn(II) atom. Such connection modes make complex **4** a 2-fold interpenetrating 3D network (Figure 6b).

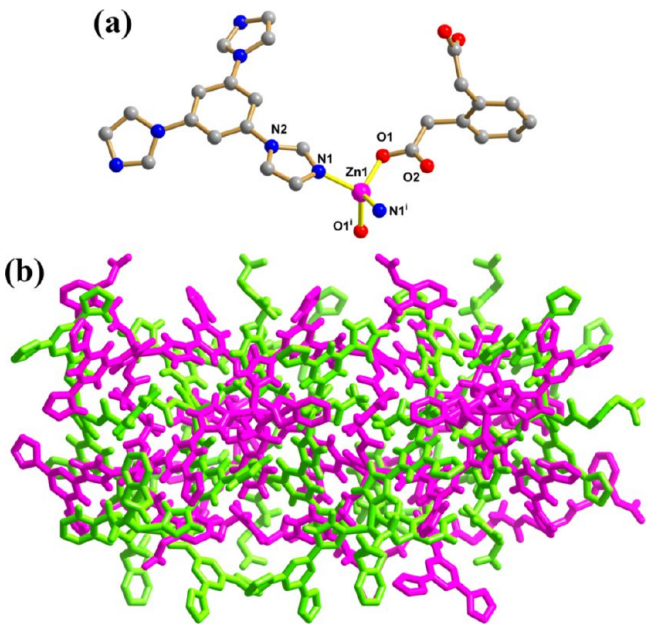

Figure 6. (a) The coordination environment of Zn(II) ions in **4** (symmetry codes: (i) $-x + 1/2, -z + 1/2, -y + 1/2$). (b) The 2-fold interpenetrating 3D network (networks individually colored).

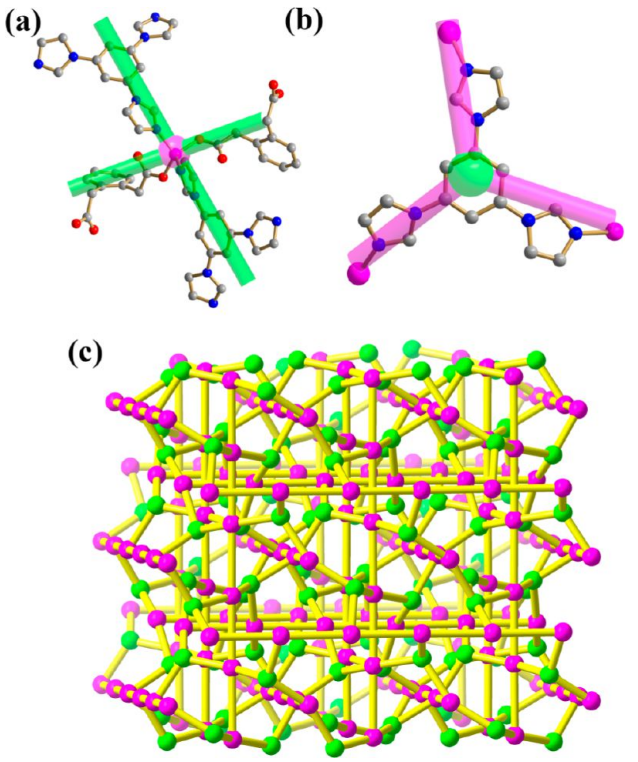

Figure 7. (a) The 4-coordinated tetrahedral Zn(II) building unit. (b) The 3-coordinated triangle tib node. (c) Ball-and-stick and schematic representations of simplified 3D 3,4-coordinated **srd** net with $\{6^3\}_2\{6^4{\cdot}9^2\}_3$ topology.

Topologically, each Zn(II) atom has been linked by four ligand, so each Zn(II) can be simplified into a 4-coordinated node (Figure 7a), while the tib still acts as a 3-coordinated linker (Figure 7b), so the resulting structure can be reduced to a binodal (3,4)-coordinated **srd** net with $\{6^3\}_2\{6^4{\cdot}9^2\}_3$ topology (Figure 7c). Two equivalent nets adopt 2-fold interpenetration to minimize the large voids in the single net. However, in spite of interpenetration, **2** still possesses free void space estimated to be about 5948.9 Å^3, that is, 12.4% of the unit cell. An analysis of the topology of interpenetration reveals that **2** also belongs to Class **II**a; that is, two interpenetrated nets are generated only by symmetry element (here is inversion center) from the single net. To the best of our knowledge, this is the first example of the **srd** topology, moreover, probably the most symmetrical embedding of 2-fold **srd** network array. The space-group symmetry of a net in the array is $F4_132$, that is, a maximal class-equivalent subgroup of the highest space-group symmetry ($P4_232$) of the single **srd** net.[20a]

*{[Zn_2(tib)$_2$(pma)]·4H_2O}$_n$ (**5**).* The single-crystal diffraction analysis indicates that complex **5** crystallized in an orthorhombic manner with space group *Pbca*. There are one Zn(II) ion, one tib ligand, half of pma ligand lying at a site of $\bar{1}$ symmetry, and two lattice water molecules in one asymmetric unit of **5**. The coordination environment around the Zn(II) atom is exhibited in Figure 8a along with the atom numbering scheme. The Zn1 is located in a slightly ZnN_3O tetrahedral geometry (τ_4 = 0.89) completed by three N atoms belonging to three tib ligands and one O atom from pma ligand (Zn1−N: 1.985(4)−2.024(4) Å; Zn1−O1 = 1.911(3) Å). Notably, the coordination enviornment of Zn(II) center in **5** (ZnN_3O tetrahedron) is completely different from that of in **1**−**4** (ZnN_2O_2 tetrahedron). Each tib ligand coordinates to three Zn(II) atoms with a nonplanar geometry with dihedral angles of 31.8(3), 12.9(3), and 27.7(3)°, respectively. On the other hand, the pma ligand is completely deprotonated but uses only two of four carboxylate groups to connect the Zn(II) atom with (κ^1)-(κ^1)-μ_2 mode. The uncoordinated carboxylate groups form hydrogen bonds with lattice water molecules. The bidentate bridging pma combines with tib to link Zn(II) centers, giving the resulting self-penetrating 3D network (Figure 8b).

The topology analysis for the 3D network of **5** is similar to that for **2** and **4** considering the 4-coordinated Zn(II) and 3-coordinated tib linker. However, different from 2-fold interpenetrating (3,4)-coordinated 3D networks of **2** and **4**, complex **5** is a self-penetrating (3,4)-coordinated new topology with point symbol of $\{10^3\}\{10^6\}$ (Figure 8c,d). We have deposited it to the TOPOS TTD Collection under the name **sun3**. Using the TOPOS cluster analysis similar to **1** and **2**, we found that the binodal (3,4)-coordinated self-penetrating network can be decomposed to two interpenetrating uninodal 3-coordinated 10^3 **srs** ($SrSi_2$) nets by omitting 2-coordinated pma ligand (Figure 8e). In this case, the 4-coordinated Zn(II) node of the **sun3** net is reduced to a 3-coordinated node in the **srs** net. The

dx.doi.org/10.1021/cg3017358 | *Cryst. Growth Des.* 2013, 13, 1277−1289

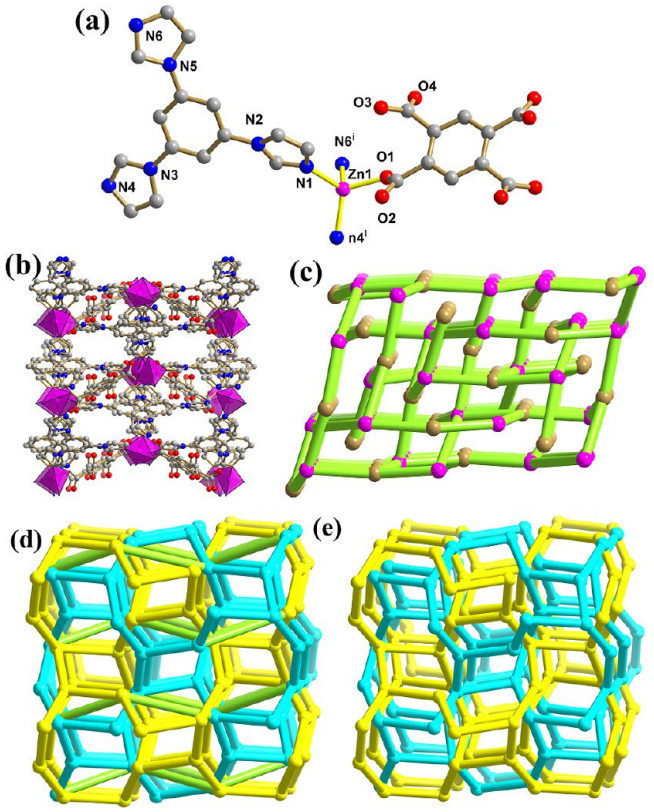

Figure 8. (a) The coordination environment of Zn(II) ion in **5**. (Symmetry codes: (i) $x - 1/2, -y + 1/2, -z + 1$; (ii) $-x + 2, y - 1/2, -z + 3/2$.) (b) The ball-and-stick representations of 3D network. (c) The simplified (3,4)-coordinated network (puple ball: 4-coordinated Zn(II) node; brown bal: 3-coordinated tib node). (d) Representations of self-penetrating network (green stick: 2-coordinated pma). (e) 2-fold interpenetrating 10^3-**srs** networks formed by breaking the green sticks in panel d.

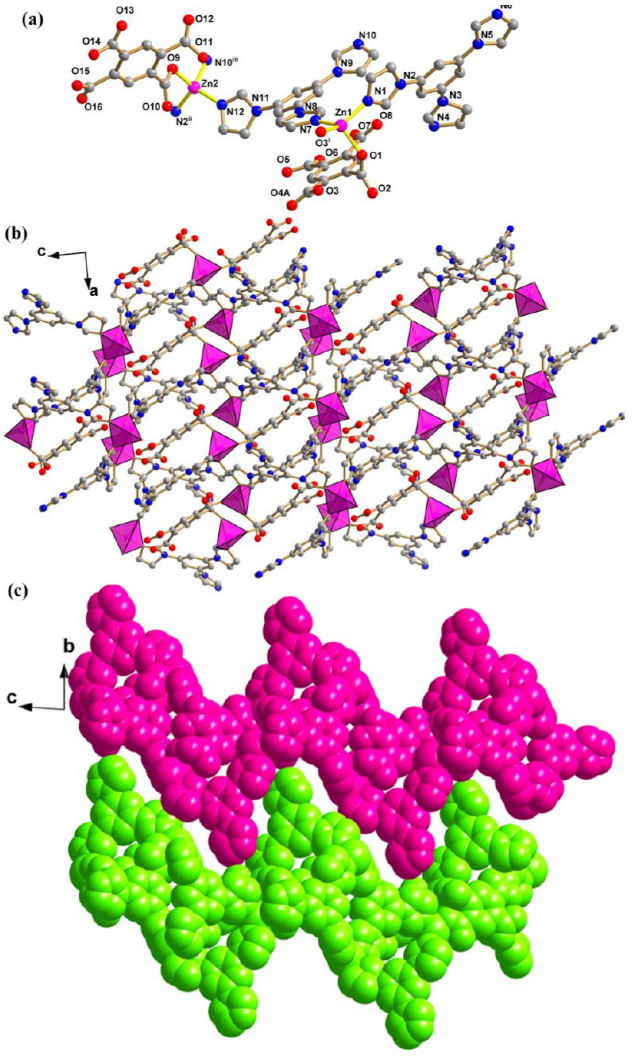

Figure 9. (a) The coordination environments of Zn(II) ions in **6**. (Symmetry codes: (i) $-x + 2, -y, -z + 1$; (ii) $-x + 1, -y, -z$; (iii) $-x, -y, -z$.) (b) The ball-and-stick representations of 2D layer viewed along the *b* axis. (c) The space-filling mode showing the 2D → 3D interdigitated networks viewed along the *a* axis (layers individually colored).

interpenetration in **5** also belongs to Class **IIa** since the two nets are related only by inversion.

{[Zn_2(tib)(Htib)(H_2pma)(Hpma)]·2H_2O}$_n$ ***(6)***. When the solvent system DMF-H_2O (v:v = 1:1) in the synthesis of **5** was replaced by DMSO-H_2O (v:v = 1:1), complex **6** was obtained as an interesting 2D → 3D interdigitated network based on 2D layers. Structural analysis indicates that complex **6** crystallizes in triclinic crystal system with space group of $P\bar{1}$. The asymmetric unit of **6** consists of two crystallographically independent Zn(II) atoms, one tib neutral ligand, one Htib cationic ligand, one H_2pma, one Hpma ligand, and two lattice water molecules. The coordination environment around the Zn(II) atoms is exhibited in Figure 9a along with the atom numbering scheme. Both Zn1 and Zn2 are in a slightly ZnN_2O_2 tetrahedral geometry with τ_4 of 0.79 and 0.92, respectively. The Zn−N and Zn−O bond lengths are in the ranges of 1.993(2)−2.013(2) and 1.9087(18)−2.025(2) Å, respectively. Two crystallographically unique N-ligands adopt two different forms, neutral tib and cationic Htib, to bind Zn(II) atoms with nonplanar geometries. Interestingly, O-ligands also show two forms, H_2pma and Hpma, depending on the degrees of deprotonation. The tib and Htib act as tri- and bidentate ligands, and combine with (κ^1)-(κ^1)-μ_2-Hpma and (κ^1)-μ_1-H_2pma to connect Zn(II) atoms to the resulting 2D undulated 3,3-coordinated layer (Figure 9b). According to the TOPOS notation,[18] the topology of the layer is 3,3L4. Notably, the protonated imidazole group of Htib and H_2pma are out of the plane 2D layer, causing the large aperture, which allowed the protuberant groups to embed, forming the resulting 2D → 3D interdigitated network (Figure 9c).

Furthermore, the lattice water molecules, Htib, Hpma, and H_2pma form O_{water}−H···$O_{carboxylate}$, $O_{carboxylate}$−H···$O_{carboxylate}$, N_{Htib}−H···O_{water} hydrogen bonds ranging from 2.376(4) to 3.112(4) Å (Table 3), which combine with $\pi\cdots\pi$ stacking interaction (3.4687(15) Å) between imidazole and phenyl ring of Hpma to reinforce the resulting 3D supramolecular framework.

Effects of Polycarboxylate Ligand and Solvent System on the Structure. Design and assembly of new CPs with novel topology and specific functionality becomes a goal being constantly pursued in the branch of the coordination chemistry field. The key strategy rests on the selection of proper organic ligands owning various geometry, length, and flexibility. Thus, in this work, we selected the rigid tripodal tib as a neutral ligand and a series of auxiliary polycarboxylates as an organic anion. Moreover, a solvent modulation strategy was also employed.

dx.doi.org/10.1021/cg3017358 | *Cryst. Growth Des.* 2013, 13, 1277−1289

Table 3. The Hydrogen Bond Geometries (Å and °) for 6[a]

D—H···A	D—H	H···A	D···A	D—H···A
O1W—H1WA···O2^{iv}	0.85	1.90	2.722(3)	162.9
O1W—H1WB···O16^{v}	0.85	2.05	2.888(4)	166.6
O2W—H2WA···O15^{vi}	0.85	2.37	3.112(4)	146.7
O2W—H2WB···O1^{vii}	0.85	1.96	2.800(3)	170.2
O7—H7A···O6	0.82	1.60	2.414(3)	173.1
O11—H11···O5^{iv}	0.82	1.83	2.642(3)	169.9
O14—H14A···O15	0.82	1.56	2.376(4)	175.9
N6—H6···O2W	0.86	1.89	2.733(3)	164.3

[a]Symmetry codes: (iv) $x-1, y, z$; (v) $x, y+1, z$; (vi) $-x, -y, -z+1$; (vii) $-x+1, -y+1, -z+1$.

From the structure description above, we can see that the polycarboxylate ligand and solvent system play important roles in the formation of the diverse structures and topologies. Six CPs contain the same tib ligand and Zn(II) center showing bi- or tridentate coordination mode and tetrahedral coordination geometry. Although different polycarboxylate ligands show the same (κ^1)-(κ^1)-μ_2 coordination mode, they have different geometries and lengths and can freely bend or rotate when coordinating to the central metals; hence they as 2-coordinated linkers extend Zn(II) centers with different orientations, which results in the different structural motifs and topologies containing the 1D SWMONT (**3**), 2D undulated layer with interdigitation feature (**6**), 3D self-catenating framework based on interpenetrating (4,6)-coordinated **sun1** subnets (**1**), 3D 2-fold interpenetrating (3,4)-coordinated networks with different topologies **sun2** and **srd** (**2** and **4**), and 3D self-penetrating (3,4)-coordinated **sun3** network based on two interpenetrating 3-coordinated 10^3 **srs** subnets (**5**). It is noteworthy that combination of 3-coordinated triangle tib node and 4-coordinated tetrahedral Zn(II) node resulted in (3,4)-coordinated networks for **2**, **4**, and **5**; however, three CPs show completely distinct topologies with point symbols ranging from $\{10^3\}_2\{10^6\}_3$, $\{6^3\}_2\{6^4{\cdot}9^2\}_3$, to $\{10^3\}\{10^6\}$. The results indicate that the different polycarboxylate anions have a remarkable effect on the structures of the CPs. Note that TOPOS cluster analysis reveals that self-catenating or interpenetrating motifs in **1**, **2**, and **5** can be unweaved by breaking a minor number of coordination bonds Zn—N or Zn—O. One can thus consider the formation of the entangled motifs as a reverse process of establishing such bonds between untangled groups already existing in the reaction media.

On the other hand, **3**/**4** and **5**/**6** exhibit the effect of the solvent systems on the resultant structures. The dimensionality and topology of the networks produced in them are determined by the coordination modes of tib and polycarboxylate anions, which are clearly dictated by the solvent molecules. For **3** and **4**, the reaction in DMF-H_2O (1 mL, v/v, 1:1) solvent results in the formation of **3**, while **4** forms in DMA-C_2H_5OH-H_2O (v:v:v = 5:2:1). The tib ligand show bidentate and tridentate modes in **3** and **4**, respectively, giving them 1D SWMONT and 3D 2-fold interpenetrating (3,4)-coordinated network with a **srd** topology. For **5** and **6**, they were obtained in DMF-H_2O (1 mL, v:v = 1:1) and DMSO-H_2O (1 mL, v:v = 1:1), respectively. In them, tib ligand shows the same coordination fashions, but the H_4pma exhibits different degree of deprotonation and binding modes. The forms of H_4pma after reaction with metal center are H_2pma for **5**, Hpma and H_2pma for **6**. The H_2pma ligand in **5** adopts a bidentate coordination mode with two carboxylate groups at 1,4-positions and contributed significantly to the formation of a self-penetrating network. Differently, the H_2pma ligand in **6** just adopts a mondentate coordination mode and contributed much less to the expansion of the dimensionality, while the triply deprotonated Hpma adopts the (κ^1)-(κ^1)-μ_2-mode using its two carboxylate groups at 1,2-positions in **6**, resulting a 2D undulated networks. Although no different solvent molecules participated in the host framework of **3**/**4** and **5**/**6**, different solvent system indeed regulates the formation of different environments for the self-assembly process and influences different degrees of deprotonation and binding modes of ligand.

Thermal Analysis. The TG analysis was performed in N_2 atmosphere on polycrystalline samples of CPs **1**—**6**, and the TG curves are shown in Figure S9. In four compounds, all CPs have two identifiable weight loss steps. For **1**, the first weight loss in the temperature range of 100—225 °C is consistent with the removal of lattice DMF and water molecule (obsd 19.15%, calcd 20.54%). The solvent-free network does not decompose until 425 °C, and then the collapse of the network of **1** occurs. For **2**, the first weight loss from 50 to 190 °C is attributed to the loss of lattice water molecules (obsd 6.35%, calcd 5.78%). Above 430 °C, it starts to lose its ligands a result of thermal decomposition. For **3**, the loss of uncoordinated water molecules (obsd 6.11%, calcd 6.32%) is observed before 140 °C. The abrupt weight loss corresponding to the release of organic ligands starts at 335 °C. For **4**, the weight loss of 4.99% from 50 to 205 °C is attributed to the loss of the free water molecules (calcd 4.44%). The weight loss corresponding to the release of organic ligands starts at 280 °C. For **5**, the first weight loss in the temperature range of 25—180 °C is consistent with the removal of lattice water molecule (obsd 14.89%, calcd 14.33%). Then the collapse of the network of **5** occurs. For **6**, the first weight loss from 50 to 190 °C is attributed to the loss of lattice water molecules (obsd 3.61%, calcd 2.94%). Then, it starts to gradually lose its ligands a result of thermal decomposition.

Photoluminescence Properties. The emission spectra of **1**—**6** were examined in the solid state at room temperature, shown in Figure S10. The free ligand tib display photoluminescence with emission maxima at 405 nm (λ_{ex} = 360 nm), assigned to $\pi^* \rightarrow \pi$ transition of tib.[34] The polycarboxylate ligands H_2bdc (λ_{em} = 358 nm), H_2bpdc (λ_{em} = 408 nm), H_2pdac (λ_{em} = 415 nm), H_4pma (λ_{em} = 337 nm) can also exhibit fluorescence at room temperature.[35] The emission bands of these polycarboxylate ligands can be assigned to the $\pi^* \rightarrow$ n transition as previously reported.[36] To the best of our knowledge, the emission of polycarboxylate belongs to $\pi^* \rightarrow$ n transitions which is very weak compared to that of the $\pi^* \rightarrow \pi$ transition of tib, so the polycarboxylates almost have no contribution to the fluorescent emission of as-synthesized CPs.[37] The emission spectra exhibit maximum emission peaks at 410 nm for **1**, 396 nm for **2**, 315, and 384 nm for **3**, 327, and 367 nm for **4**, and 392, 408, and 465 nm for **5**, and 467 nm for **6**, respectively, under the exciation at 300 nm. According to the literature, the Zn(II) ion is difficult to oxidize or reduce because of the d^{10} configuration. As a result, the emissions of these CPs are neither metal-to-ligand charge transfer (MLCT) nor ligand-to-metal charge transfer (LMCT) in nature.[38] Thus, they may be assigned to a mixture characteristics of intraligand and ligand-to-ligand charge transition (LLCT), as reported for other Zn(II) CPs constructed from mixed N-donor and O-donor ligands.[39] The enhancement of luminescence in d^{10} complexes may be attributed to ligand chelation to the metal center which

dx.doi.org/10.1021/cg3017358 | Cryst. Growth Des. 2013, 13, 1277—1289

effectively increases the rigidity of the ligand and reduces the loss of energy by radiationless decay.[40] The difference of the emission behaviors for **1**−**6** probably derive from the differences in the rigidity of solid-state crystal packing.

CONCLUSIONS

In conclusion, six new Zn(II) CPs constructed from a tripodal imidazole-based tridentate ligand and different polycarboxylates have been successfully obtained under solvothermal conditions. By using different polycarboxylates as the secondary ligands, a self-catenating 3D framework (**1**) based on two interpenetrating (4,6)-coordinated **sun1** subnets, a 2-fold interpenetrating 3D (3,4)-coordinated new topology **sun2** with point symbol of $\{10^3\}_2\{10^6\}_3$ (**2**), an interesting 1D independent single-wall metal−organic nanotube (**3**), and a 3D (3,4)-coordinated self-penetrating network **sun3** with point symbol of $\{10^3\}\{10^6\}$ (**5**) have been obtained. By changing the solvent systems in the synthesis of **3** and **5**, another 2-fold interpenetrating 3D (3,4)-coordinated network with a **srd** topology (**4**) and an undulated 2D layer 3,3L4 (**6**) were obtained. The results indicate that the introduction of polycarboxylate ligands with different geometry, length, and flexibility as well as the solvent system show significant effects on the formation of the resulting structures.

ASSOCIATED CONTENT

Supporting Information

Crystallographic data in CIF format, IR, powder X-ray diffraction (PXRD) patterns for **1**−**6**. CCDC 910564−910569. This material is available free of charge via the Internet at http://pubs.acs.org.

AUTHOR INFORMATION

Corresponding Author

*E-mail: dsun@sdu.edu.cn (D.S); blatov@samsu.ru (V.A.B).

Notes

The authors declare no competing financial interest.

ACKNOWLEDGMENTS

This work was supported by the NSFC (Grant No. 21201110), Independent Innovation Foundation of Shandong University (2011GN030), the Special Fund for Postdoctoral Innovation Program of Shandong Province (201101007), and the China Postdoctoral Science Foundation (2012M511492).

REFERENCES

(1) (a) Kong, X.-J.; Long, L.-S.; Zheng, Z.; Huang, R.-B.; Zheng, L.-S. *Acc. Chem. Res.* **2010**, *43*, 201. (b) Rusanov, E. B.; Ponomarova, V. V.; Komarchuk, V. V.; Stoeckli-Evans, H.; Fernandez-Ibanez, E.; Stoeckli, F.; Sieler, J.; Domasevitch, K. V. *Angew. Chem., Int. Ed.* **2003**, *42*, 2499. (c) Zhao, D.; Tan, S. W.; Yuan, D. Q.; Lu, W. G.; Rezenom, Y. H.; Jiang, H. L.; Wang, L. Q.; Zhou, H. C. *Adv. Mater.* **2011**, *23*, 90. (d) Chen, B.; Xiang, S.; Qian, G. *Acc. Chem. Res.* **2010**, *43*, 1115. (e) Yoshizawa, M.; Klosterman, J. K.; Fujita, M. *Angew. Chem., Int. Ed.* **2009**, *48*, 3418. (f) Zhao, D.; Yuan, D. Q.; Zhou, H. C. *Energ. Environ. Sci.* **2008**, *1*, 222. (g) Chen, L.; Jiang, F.; Lin, Z.; Zhou, Y.; Yue, C.; Hong, M. *J. Am. Chem. Soc.* **2005**, *127*, 8588. (h) Zeng, M. H.; Yao, M. X.; Liang, H.; Zhang, W. X.; Chen, X. M. *Angew. Chem., Int. Ed.* **2007**, *46*, 1832. (i) Yaghi, O. M.; Tranchemontagne, D. J.; Mendoza-Cortes, J. L.; O'Keeffe, M. *Chem. Soc. Rev.* **2009**, *38*, 1257. (j) Liu, Q. K.; Ma, J. P.; Dong, Y. B. *J. Am. Chem. Soc.* **2010**, *132*, 7005. (k) Kong, X.-J.; Ren, Y.-P.; Long, L.-S.; Zheng, Z.; Huang, R.-B.; Zheng, L.-S. *J. Am. Chem. Soc.* **2007**, *129*, 7016. (l) Kong, X.-J.; Wu, Y.; Long, L.-S.; Zheng, L.-S.; Zheng, Z. *J. Am. Chem. Soc.* **2009**, *131*, 6918. (m) Xuan, W. M.; Zhang, M. N.; Liu, Y.; Chen, Z. J.; Cui, Y. *J. Am. Chem. Soc.* **2012**, *134*, 6904. (n) Wu, H.; Yang, J.; Su, Z. M.; Batten, S. R.; Ma, J. F. *J. Am. Chem. Soc.* **2011**, *133*, 11406. (o) Gao, E. Q.; Yue, Y. F.; Bai, S. Q.; He, Z.; Yan, C. H. *J. Am. Chem. Soc.* **2004**, *126*, 1419. (p) Chen, X.; Li, H. X.; Zhang, Z. Y.; Zhao, W.; Lang, J. P.; Abrahams, B. F. *Chem. Commun.* **2012**, *48*, 4480. (q) O'Keeffe, M.; Yaghi, O. M. *Chem. Rev.* **2012**, *112*, 675. (r) Janiak, C.; Vieth, J. K. *New J. Chem.* **2010**, *34*, 2366.

(2) (a) Yuan, D. Q.; Zhao, D.; Sun, D. F.; Zhou, H. C. *Angew. Chem., Int. Ed.* **2010**, *49*, 5357. (b) Domasevitch, K. V.; Solntsev, P. V.; Gural'skiy, I. A.; Krautscheid, H.; Rusanov, E. B.; Chernega, A. N.; Howard, J. A. K. *Dalton Trans.* **2007**, 3893. (c) Sun, D. F.; Ma, S. Q.; Ke, Y. X.; Collins, D. J.; Zhou, H. C. *J. Am. Chem. Soc.* **2006**, *128*, 3896. (d) Tanabe, K. K.; Allen, C. A.; Cohen, S. M. *Angew. Chem., Int. Ed.* **2010**, *49*, 9730. (e) Su, C.-Y.; Cai, Y.-P.; Chen, C.-L.; Smith, M. D.; Kaim, W.; Zur Loye, H.-C. *J. Am. Chem. Soc.* **2003**, *125*, 8595. (f) Perry, J. J.; Perman, J. A.; Zaworotko, M. J. *Chem. Soc. Rev.* **2009**, *38*, 1400. (g) Moulton, B.; Zaworotko, M. J. *Chem. Rev.* **2001**, *101*, 1629. (h) Yin, Z.; Wang, Q. X.; Zeng, M. H. *J. Am. Chem. Soc.* **2012**, *134*, 4857. (i) Zeng, M. H.; Wang, Q. X.; Tan, Y. X.; Hu, S.; Zhao, H. X.; Long, L. S.; Kurmoo, M. *J. Am. Chem. Soc.* **2010**, *132*, 2561. (j) Zeng, M. H.; Zhang, W. X.; Sun, X. Z.; Chen, X. M. *Angew. Chem., Int. Ed.* **2005**, *44*, 3079. (k) Zhao, D.; Yuan, D. Q.; Sun, D. F.; Zhou, H. C. *J. Am. Chem. Soc.* **2009**, *131*, 9186. (l) Yuan, D. Q.; Zhao, D.; Timmons, D. J.; Zhou, H. C. *Chem. Sci.* **2011**, *2*, 103. (m) Bi, Y. F.; Wang, X. T.; Liao, W. P.; Wang, X. F.; Wang, X. W.; Zhang, H. J.; Gao, S. *J. Am. Chem. Soc.* **2009**, *131*, 11650. (n) Zhou, X. P.; Liu, J.; Zhan, S. Z.; Yang, J. R.; Li, D.; Ng, K. M.; Sun, R. W. Y.; Che, C. M. *J. Am. Chem. Soc.* **2012**, *134*, 8042. (o) Zhou, X. P.; Li, M.; Liu, J.; Li, D. *J. Am. Chem. Soc.* **2012**, *134*, 67. (p) Fu, J. H.; Li, H. J.; Mu, Y. J.; Hou, H. W.; Fan, Y. T. *Chem. Commun.* **2011**, *47*, 5271.

(3) (a) Zhao, D.; Timmons, D. J.; Yuan, D.; Zhou, H.-C. *Acc. Chem. Res.* **2011**, *44*, 123. (b) Yaghi, O. M. *Nat. Mater.* **2007**, *6*, 92. (c) Maji, T. K.; Matsuda, R.; Kitagawa, S. *Nat. Mater.* **2007**, *6*, 142. (d) Kitagawa, S.; Kitaura, R.; Noro, S. *Angew. Chem., Int. Ed.* **2004**, *43*, 2334. (e) Aromi, G.; Berzal, P. C.; Gamez, P.; Roubeau, O.; Kooijman, H.; Spek, A. L.; Driessen, W. L.; Reedijk, J. *Angew. Chem., Int. Ed.* **2001**, *40*, 3444. (f) Bi, W. H.; Cao, R.; Sun, D. F.; Yuan, D. Q.; Li, X.; Wang, Y. Q.; Li, X. J.; Hong, M. C. *Chem. Commun.* **2004**, 2104. (g) Qiu, W.; Perman, J. A.; Wojtas, L.; Eddaoudi, M.; Zaworotko, M. J. *Chem. Commun.* **2010**, *46*, 8734. (h) Sun, D.; Yan, Z.-H.; Liu, M.; Xie, H.; Yuan, S.; Lu, H.; Feng, S.; Sun, D. *Cryst. Growth Des.* **2012**, *12*, 2902.

(4) (a) Wu, H. B.; Huang, Z. J.; Wang, Q. M. *Chem.—Eur. J.* **2010**, *16*, 12321. (b) Qiao, J.; Shi, K.; Wang, Q.-M. *Angew. Chem., Int. Ed.* **2010**, *49*, 1765. (c) Li, G.; Lei, Z.; Wang, Q.-M. *J. Am. Chem. Soc.* **2010**, *132*, 17678. (d) Wu, H.-B.; Wang, Q.-M. *Angew. Chem., Int. Ed.* **2009**, *48*, 7343. (e) Jia, J.-H.; Wang, Q.-M. *J. Am. Chem. Soc.* **2009**, *131*, 16634. (f) Lee, J. Y.; Kim, H. J.; Park, C. S.; Sim, W.; Lee, S. S. *Chem.—Eur. J.* **2009**, *15*, 8989.

(5) (a) Chen, M.; Chen, S.-S.; Okamura, T.-a.; Su, Z.; Chen, M.-S.; Zhao, Y.; Sun, W.-Y.; Ueyama, N. *Cryst. Growth Des.* **2011**, *11*, 1901. (b) Li, B.; Wei, R. J.; Tao, J.; Huang, R. B.; Zheng, L. S.; Zheng, Z. P. *J. Am. Chem. Soc.* **2010**, *132*, 1558. (c) Fang, S. M.; Zhang, Q.; Hu, M.; Sanudo, E. C.; Du, M.; Liu, C. S. *Inorg. Chem.* **2010**, *49*, 9617. (d) Su, Z.; Fan, J.; Okamura, T.; Sun, W. Y.; Ueyama, N. *Cryst. Growth Des.* **2010**, *10*, 3515. (e) Sun, D.; Wei, Z. H.; Wang, D. F.; Zhang, N.; Huang, R. B.; Zheng, L. S. *Cryst. Growth. Des.* **2011**, *11*, 1427. (f) Long, L.-S. *CrystEngComm* **2010**, *12*, 1354. (g) Li, C.-P.; Du, M. *Chem. Commun.* **2011**, *47*, 5958. (h) Sun, D.; Li, Y.-H.; Hao, H.-J.; Liu, F.-J.; Wen, Y.-M.; Huang, R.-B.; Zheng, L.-S. *Cryst. Growth Des.* **2011**, *11*, 3323. (i) Sun, D.; Wei, Z. H.; Yang, C. F.; Wang, D. F.; Zhang, N.; Huang, R. B.; Zheng, L. S. *CrystEngComm* **2011**, *13*, 1591. (j) Lee, S. Y.; Jung, J. H.; Vittal, J. J.; Lee, S. S. *Cryst. Growth Des.* **2010**, *10*, 1033.

(6) (a) Masaoka, S.; Tanaka, D.; Nakanishi, Y.; Kitagawa, S. *Angew. Chem., Int. Ed.* **2004**, *43*, 2530. (b) Sun, D. F.; Ke, Y. X.; Mattox, T. M.; Ooro, B. A.; Zhou, H. C. *Chem. Commun.* **2005**, 5447. (c) Chen, S.-S.; Chen, M.; Takamizawa, S.; Chen, M.-S.; Su, Z.; Sun, W.-Y. *Chem. Commun.* **2011**, *47*, 752. (d) Zhuang, C.-F.; Zhang, J.; Wang, Q.; Chu, Z.-H.; Fenske, D.; Su, C.-Y. *Chem.—Eur. J.* **2009**, *15*, 7578. (e) Sun, D.; Liu, F.-J.; Huang, R.-B.; Zheng, L.-S. *Inorg. Chem.* **2011**, *50*, 12393.

(f) Wang, X. Y.; Wang, L.; Wang, Z. M.; Gao, S. *J. Am. Chem. Soc.* **2006**, *128*, 674.
(7) (a) Fan, J.; Gan, L.; Kawaguchi, H.; Sun, W. Y.; Yu, K. B.; Tang, W. X. *Chem.—Eur. J.* **2003**, *9*, 3965. (b) Su, Z.; Fan, J.; Okamura, T.; Sun, W. Y.; Ueyama, N. *Cryst. Growth Des.* **2010**, *10*, 3515. (c) Xu, J.; Pan, Z. R.; Wang, T. W.; Li, Y. Z.; Guo, Z. J.; Batten, S. R.; Zheng, H. G. *CrystEngComm* **2010**, *12*, 612. (d) Wang, X. F.; Lv, Y.; Okamura, T. A.; Kawaguchi, H.; Wu, G.; Sun, W. Y.; Ueyama, N. *Cryst. Growth Des.* **2007**, *7*, 1125. (e) Su, Z.; Chen, M. S.; Fan, J. A.; Chen, M.; Chen, S. S.; Luo, L.; Sun, W. Y. *CrystEngComm* **2010**, *12*, 2040. (f) Su, Z.; Song, Y.; Bai, Z. S.; Fan, J. A.; Liu, G. X.; Sun, W. Y. *CrystEngComm* **2010**, *12*, 4339. (g) Fan, J.; Sun, W. Y.; Okamura, T.; Tang, W. X.; Ueyama, N. *Inorg. Chem.* **2003**, *42*, 3168. (h) Cha, Y. E.; Ma, X.; Li, X.; Shi, H. Z.; Tan, H. L.; Meng, Y. *Inorg. Chem. Commun.* **2012**, *20*, 108. (i) Su, Z.; Wang, Z. B.; Sun, W. Y. *Inorg. Chem. Commun.* **2010**, *13*, 1278. (j) Wang, X.; Peng, J.; Wang, D. D.; Liu, M. G.; Meng, C. L.; Tian, A. X.; Alimaje, K.; Shi, Z. Y. *Inorg. Chim. Acta* **2012**, *392*, 160. (k) Zhao, W.; Fan, H.; Okamura, T.; Sun, W. Y.; Ueyama, N. *Microporous Mesoporous Mater.* **2005**, *78*, 265. (l) Rit, A.; Pape, T.; Hepp, A.; Hahn, F. E. *Organometallics* **2011**, *30*, 334. (m) Li, L.; Fan, J.; Okamura, T. A.; Li, Y. Z.; Sun, W. Y.; Ueyama, N. *Supramol. Chem.* **2004**, *16*, 361. (n) Ji, C. C.; Li, J.; Li, Y. Z.; Guo, Z. J.; Zheng, H. G. *CrystEngComm* **2011**, *13*, 459. (o) Pan, Z. R.; Yao, X. Q.; Zheng, H. G.; Li, Y. Z.; Guo, Z. J.; Batten, S. R. *CrystEngComm* **2009**, *11*, 605.
(8) (a) Cui, P.; Wu, J.; Zhao, X.; Sun, D.; Zhang, L.; Guo, J.; Sun, D. *Cryst. Growth Des.* **2011**, *11*, 5182. (b) Xu, B.; Lin, X.; He, Z. Z.; Lin, Z. J.; Cao, R. *Chem. Commun.* **2011**, *47*, 3766. (c) Wang, S. N.; Bai, J. F.; Li, Y. Z.; Pan, Y.; Scheer, M.; You, X. Z. *CrystEngComm* **2007**, *9*, 1084. (d) Seo, J.; Matsuda, R.; Sakamoto, H.; Bonneau, C.; Kitagawa, S. *J. Am. Chem. Soc.* **2009**, *131*, 12792. (e) Sun, D.; Hao, H.-J.; Liu, F.-J.; Su, H.-F.; Huang, R.-B.; Zheng, L.-S. *CrystEngComm* **2012**, *14*, 480. (f) Sun, D.; Li, Y.-H.; Hao, H.-J.; Liu, F.-J.; Zhao, Y.; Huang, R.-B.; Zheng, L.-S. *CrystEngComm* **2011**, *13*, 6431. (g) Sun, D.; Li, Y.-H.; Wu, S.-T.; Hao, H.-J.; Liu, F.-J.; Huang, R.-B.; Zheng, L.-S. *CrystEngComm* **2011**, *13*, 7311. (h) Sun, D.; Wei, Z. H.; Yang, C. F.; Wang, D. F.; Zhang, N.; Huang, R. B.; Zheng, L. S. *CrystEngComm* **2011**, *13*, 1591. (i) Sun, D.; Xu, Q.-J.; Ma, C.-Y.; Zhang, N.; Huang, R.-B.; Zheng, L.-S. *CrystEngComm* **2010**, *12*, 4161. (j) Hu, J. S.; Shang, Y. J.; Yao, X. Q.; Qin, L.; Li, Y. Z.; Guo, Z. J.; Zheng, H. G.; Xue, Z. L. *Cryst. Growth Des.* **2010**, *10*, 4135. (k) Ji, C. C.; Li, J.; Li, Y. Z.; Guo, Z. J.; Zheng, H. G. *CrystEngComm* **2011**, *13*, 459. (l) Chen, Z.; Gao, D. L.; Diao, C. H.; Liu, Y.; Ren, J.; Chen, J.; Zhao, B.; Shi, W.; Cheng, P. *Cryst Growth Des* **2012**, *12*, 1201. (m) Liu, C.-S.; Shi, X.-S.; Li, J.-R.; Wang, J.-J.; Bu, X.-H. *Cryst. Growth Des.* **2006**, *6*, 656. (n) Zhang, L. Y.; Zhang, J. P.; Lin, Y. Y.; Chen, X. M. *Cryst. Growth Des.* **2006**, *6*, 1684. (o) Matsuda, R.; Kitaura, R.; Kitagawa, S.; Kubota, Y.; Kobayashi, T. C.; Horike, S.; Takata, M. *J. Am. Chem. Soc.* **2004**, *126*, 14063.
(9) (a) Zou, R. Q.; Zhong, R. Q.; Du, M.; Kiyobayashi, T.; Xu, Q. *Chem. Commun.* **2007**, 2467. (b) Carlucci, L.; Ciani,G.; Proserpio, D. M. *Networks, Topologies, and Entanglements. In Making Crystals by Design-Methods, Techniques and Applications*; Braga, D., Grepioni, F., Eds.; Wiley-VCH: Weinheim, 2007; Chapter 1.3. (c) Natarajan, R.; Savitha, G.; Dominiak, P.; Wozniak, K.; Moorthy, J. N. *Angew. Chem., Int. Ed.* **2005**, *44*, 2115. (d) Carlucci, L.; Ciani, G.; Proserpio, D. M. *Coord. Chem. Rev.* **2003**, *246*, 247. (e) Batten, S. R.; Robson, R. *Angew. Chem., Int. Ed.* **1998**, *37*, 1460. (f) Batten, S. R. *CrystEngComm* **2001**, *3*, 67. (g) Zaworotko, M. J. *Chem. Commun.* **2001**, 861.
(10) (a) Lan, Y.; Wang, X.; Li, S.; Su, Z.; Shao, K.; Wang, E. *Chem. Commun.* **2007**, 4863. (b) Jia, Q.-X.; Wang, Y.-Q.; Yue, Q.; Wang, Q.-L.; Gao, E.-Q. *Chem. Commun.* **2008**, 4894. (c) Carlucci, L.; Ciani, G.; Proserpio, D. M.; Porta, F. *Angew. Chem., Int. Ed.* **2003**, *42*, 317. (d) Tong, M. L.; Chen, X. M.; Batten, S. R. *J. Am. Chem. Soc.* **2003**, *125*, 16170. (e) Xiao, D. R.; Li, Y. G.; Wang, E. B.; Fan, L. L.; An, H. Y.; Su, Z. M.; Xu, L. *Inorg. Chem.* **2007**, *46*, 4158. (f) Wang, C. Y.; Wilseck, Z. M.; LaDuca, R. L. *Inorg. Chem.* **2011**, *50*, 8997. (g) Manson, J. L.; Gu, J. Y.; Schlueter, J. A.; Wang, H. H. *Inorg. Chem.* **2003**, *42*, 3950.
(11) *SMART, SAINT and SADABS*; Bruker AXS Inc.: Madison, Wisconsin, USA, 1998.
(12) Sheldrick, G. M. *SHELXS-97, Program for X-ray Crystal Structure Determination*; University of Gottingen: Germany, 1997.
(13) Sheldrick, G. M. *SHELXL-97, Program for X-ray Crystal Structure Refinement*; University of Gottingen: Germany, 1997.
(14) Spek, A. L. *Implemented as the PLATON Procedure, a Multipurpose Crystallographic Tool*; Utrecht University; Utrecht, The Netherlands, 1998.
(15) Blatov, V. A. *Struct. Chem.* **2012**, *23*, 955 TOPOS software is available for download at http://www.topos.samsu.ru.
(16) Nakamoto, K. *Infrared and Raman Spectra of Inorganic and Coordination Compounds*;, John Wiley & Sons: New York, 1986.
(17) Yang, L.; Powell, D. R.; Houser, R. P. *Dalton Trans.* **2007**, 955.
(18) (a) He, H.; Collins, D.; Dai, F.; Zhao, X.; Zhang, G.; Ma, H.; Sun, D. *Cryst. Growth Des.* **2010**, *10*, 895. (b) Hu, T.; Bi, W.; Hu, X.; Zhao, X.; Sun, D. *Cryst. Growth Des.* **2010**, *10*, 3324. (c) Zhao, X.; He, H.; Hu, T.; Dai, F.; Sun, D. *Inorg. Chem.* **2009**, *48*, 8057. (d) He, H.; Dai, F.; Sun, D. *Dalton Trans.* **2009**, 763. (e) Zhao, X.; He, H.; Dai, F.; Sun, D.; Ke, Y. *Inorg. Chem.* **2010**, *49*, 8650.
(19) Alexandrov, E. V.; Blatov, V. A.; Kochetkov, A. V.; Proserpio, D. M. *CrystEngComm* **2011**, *13*, 3947.
(20) (a) O'Keeffe, M.; Peskov, M. A.; Ramsden, S. J.; Yaghi, O. M. *Acc. Chem. Res.* **2008**, *41*, 1782 database available at http://rcsr.anu.edu.au/. (b) Ramsden, S. J.4; Robins, V.; Hyde, S. T. *Acta Crystallogr.* **2009**, *A65*, 81 database available at http://epinet.anu.edu.au.
(21) Blatov, V. A.; Carlucci, L.; Ciani, G.; Proserpio, D. M. *CrystEngComm* **2004**, *6*, 377.
(22) Su, Z.; Xu, J.; Fan, J.; Liu, D. J.; Chu, Q.; Chen, M. S.; Chen, S. S.; Liu, G. X.; Wang, X. F.; Sun, W. Y. *Cryst. Growth Des.* **2009**, *9*, 2801.
(23) Zhao, W.; Song, Y.; Okamura, T.-a.; Fan, J.; Sun, W. Y.; Ueyama, N. *Inorg. Chem.* **2005**, *44*, 3330.
(24) (a) Huang, Y. G.; Mu, B.; Schoenecker, P. M.; Carson, C. G.; Karra, J. R.; Cai, Y.; Walton, K. S. *Angew. Chem., Int. Ed.* **2011**, *50*, 436. (b) Jung, S.; Cho, W.; Lee, H. J.; Oh, M. *Angew. Chem., Int. Ed.* **2009**, *48*, 1459. (c) Kennedy, S.; Karotsis, G.; Beavers, C. M.; Teat, S. J.; Brechin, E. K.; Dalgarno, S. *Angew. Chem., Int. Ed.* **2010**, *49*, 4205. (d) Luo, T. T.; Wu, H. C.; Jao, Y. C.; Huang, S. M.; Tseng, T. W.; Wen, Y. S.; Lee, G. H.; Peng, S. M.; Lu, K. L. *Angew. Chem., Int. Ed.* **2009**, *48*, 9461.
(25) (a) Hong, M. C.; Zhao, Y. J.; Su, W. P.; Cao, R.; Fujita, M.; Zhou, Z. Y.; Chan, A. S. C. *Angew. Chem., Int. Ed.* **2000**, *39*, 2468. (b) Wang, R. H.; Hong, M. C.; Luo, J. H.; Cao, R.; Weng, J. B. *Chem. Commun.* **2003**, 1018.
(26) Su, C. Y.; Goforth, A. M.; Smith, M. D.; Pellechia, P. J.; zur Loye, H. C. *J. Am. Chem. Soc.* **2004**, *126*, 3576.
(27) Luo, T. T.; Wu, H. C.; Jao, Y. C.; Huang, S. M.; Tseng, T. W.; Wen, Y. S.; Lee, G. H.; Peng, S. M.; Lu, K. L. *Angew. Chem., Int. Ed.* **2009**, *48*, 9461.
(28) (a) Xiang, S. L.; Huang, J.; Li, L.; Zhang, J. Y.; Jiang, L.; Kuang, X. J.; Su, C. Y. *Inorg. Chem.* **2011**, *50*, 1743. (b) Huang, X. C.; Luo, W.; Shen, Y. F.; Lin, X. J.; Li, D. *Chem. Commun.* **2008**, 3995.
(29) (a) Panda, T.; Kundu, T.; Banerjee, R. *Chem Commun* **2012**, *48*, 5464. (b) Wang, R. H.; Hong, M. C.; Luo, J. H.; Cao, R.; Weng, J. B. *Chem. Commun.* **2003**, 1018. (c) Huang, K. L.; Liu, X.; Chen, X.; Wang, D. Q. *Cryst Growth Des* **2009**, *9*, 1646. (d) Jin, J. C.; Wang, Y. Y.; Liu, P.; Liu, R. T.; Ren, C.; Shi, Q. Z. *Cryst Growth Des* **2010**, *10*, 2029. (e) Bu, F.; Xiao, S. J. *CrystEngComm* **2010**, *12*, 3385. (f) Li, B.; Chen, S. W.; Chen, Z.; Chen, J.; Guo, J. Z.; Liu, L. *CrystEngComm* **2011**, *13*, 6610. (g) Ren, S. B.; Yang, X. L.; Zhang, J.; Li, Y. Z.; Zheng, Y. X.; Du, H. B.; You, X. Z. *CrystEngComm* **2009**, *11*, 246. (h) Zhao, X. L.; Sun, D.; Hu, T. P.; Yuan, S.; Gu, L. C.; Cong, H. J.; He, H. Y.; Sun, D. F. *Dalton Trans.* **2012**, *41*, 4320. (i) Dai, F. N.; He, H. Y.; Sun, D. F. *Inorg. Chem.* **2009**, *48*, 4613. (j) Fang, C.; Liu, Q. K.; Ma, J. P.; Dong, Y. B. *Inorg. Chem.* **2012**, *51*, 3923. (k) Dai, F. N.; He, H. Y.; Sun, D. F. *J. Am. Chem. Soc.* **2008**, *130*, 14064.
(30) Dong, Y. B.; Jiang, Y. Y.; Li, J.; Ma, J. P.; Liu, F. L.; Tang, B.; Huang, R. Q.; Batten, S. R. *J. Am. Chem. Soc.* **2007**, *129*, 4520.
(31) Fan, J.; Zhu, H. F.; Okamura, T. A.; Sun, W. Y.; Tang, W. X.; Ueyama, N. *Inorg. Chem.* **2003**, *42*, 158.

(32) Tei, Z. F.; Zhao, D. B.; Geldbach, T. J.; Scopelliti, R.; Dyson, P. J.; Antonijevic, S.; Bodenhausen, G. *Angew. Chem., Int. Ed.* **2005**, *44*, 5720.
(33) Xia, J.; Shi, W.; Chen, X. Y.; Wang, H. S.; Cheng, P.; Liao, D. Z.; Yan, S. P. *Dalton Trans.* **2007**, 2373.
(34) Zhang, L.; Li, Z. J.; Lin, Q. P.; Qin, Y. Y.; Zhang, J.; Yin, P. X.; Cheng, J. K.; Yao, Y. G. *Inorg. Chem.* **2009**, *48*, 6517.
(35) (a) Sun, D.; Zhang, N.; Huang, R.-B.; Zheng, L.-S. *Cryst. Growth Des.* **2010**, *10*, 3699. (b) Sun, D.; Zhang, N.; Luo, G. G.; Xu, Q. J.; Huang, R. B.; Zheng, L. S. *Polyhedron* **2010**, *29*, 1842. (c) Yang, G.-P.; Wang, Y.-Y.; Zhang, W.-H.; Fu, A.-Y.; Liu, R.-T.; Lermontova, E. Kh.; Shi, Q.-Z. *CrystEngComm* **2010**, *12*, 1509.
(36) (a) Li, S.-L.; Lan, Y.-Q.; Ma, J.-F.; Fu, Y.-M.; Yang, J.; Ping, G.-J.; Liu, J.; Su, Z.-M. *Cryst. Growth Des.* **2008**, *8*, 1610. (b) Zhang, J.; Li, Z.-J.; Kang, Y.; Cheng, J.-K.; Yao, Y.-G. *Inorg. Chem.* **2004**, *43*, 8085. (c) Li, S.-L.; Lan, Y.-Q.; Ma, J.-F.; Yang, J.; Wei, G.-H.; Zhang, L.-P.; Su, Z.-M. *Cryst. Growth Des.* **2008**, *8*, 675.
(37) Chen, W. J.; Wang, Y.; Chen, C.; Yue, Q.; Yuan, H. M.; Chen, J. S.; Wang, S. N. *Inorg. Chem.* **2003**, *42*, 944−946.
(38) (a) Wen, L.; Li, Y.; Lu, Z.; Lin, J.; Duan, C.; Meng, Q. *Cryst. Growth Des.* **2006**, *6*, 530. (b) Wen, L.; Lu, Z.; Lin, J.; Tian, Z.; Zhu, H.; Meng, Q. *Cryst. Growth Des.* **2007**, *7*, 93. (c) Zhang, L.-P.; Ma, J.-F.; Yang, J.; Pang, Y.-Y.; Ma, J.-C. *Inorg. Chem.* **2010**, *49*, 1535.
(39) Su, Z.; Fan, J.; Okamura, T.; Chen, M.-S.; Chen, S.-S.; Sun, W.-Y.; Ueyama, N. *Cryst. Growth Des.* **2010**, *10*, 1911.21.
(40) (a) Sun, D.; Yan, Z.-H.; Liu, M.; Xie, H.; Yuan, S.; Lu, H.; Feng, S.; Sun, D. *Cryst. Growth Des.* **2012**, *12*, 290. (b) Sun, D.; Xu, H.-R.; Yang, C.-F.; Wei, Z.-H.; Zhang, N.; Huang, R.-B.; Zheng, L.-S. *Cryst. Growth Des.* **2010**, *10*, 4642. (c) Zhang, S. Q.; Jiang, F. L.; Wu, M. Y.; Ma, J.; Bu, Y.; Hong, M. C. *Cryst. Growth Des.* **2012**, *12*, 1452. (d) Wu, X. T.; Zhu, Q. L.; Sheng, T. L.; Fu, R. B.; Hu, S. M.; Chen, L.; Shen, C. J.; Ma, X. *Chem.—Eur. J.* **2011**, *17*, 3358. (e) Zheng, S.-L.; Chen, X.-M. *Aust. J. Chem.* **2004**, *57*, 703. (f) Zheng, S.-L.; Yang, J.-H.; Yu, X.-L.; Chen, X.-M.; Wong, W. T. *Inorg. Chem.* **2004**, *43*, 830.